

Sparse Functional Principal Component Analysis in High Dimensions

Xiaoyu Hu and Fang Yao

School of Mathematical Sciences, Center for Statistical Science, Peking University, China

Abstract

Functional principal component analysis (FPCA) is a fundamental tool and has attracted increasing attention in recent decades, while existing methods are restricted to data with a small number of random functions. In this work, we focus on high-dimensional functional processes where the number of random functions p is comparable to, or even much larger than the sample size n . Such data are ubiquitous in various fields such as neuroimaging analysis, and cannot be properly modeled by existing methods. We propose a new algorithm, called sparse FPCA, which is able to model principal eigenfunctions effectively under sensible sparsity regimes. While sparsity assumptions are standard in multivariate statistics, they have not been investigated in the complex context where not only is p large, but also each variable itself is an intrinsically infinite-dimensional process. The sparsity structure motivates a thresholding rule that is easy to compute without smoothing operations by exploiting the relationship between univariate orthonormal basis expansions and multivariate Karhunen-Loève (K-L) representations. We investigate the theoretical properties of the resulting estimators under two sparsity regimes, and simulated and real data examples are provided to offer empirical support which also performs well in subsequent analysis such as classification.

KEYWORDS: Basis expansion, Multivariate Karhunen-Loève expansion, Sparsity regime.

1. INTRODUCTION

Functional data have been commonly encountered in modern statistics, and dimension reduction plays a key role due to the infinite dimensionality of such data. As an important tool

for dimension reduction, FPCA is optimal in the sense that the integrated mean squared error is efficiently minimized, which has wide applications in functional regression, classification and clustering (Rice and Silverman, 1991; Yao et al., 2005a,b; Müller et al., 2005; Hall and Horowitz, 2007; Dai et al., 2017; Wong et al., 2019). Despite progress being made in this field, existing methods often involve a single or small number of random functions. In this paper, we focus on modeling principal eigenfunctions of p random functions where p is comparable to, or even much larger than the sample size n , i.e., the number of subjects. Such data, which are referred to as the high-dimensional functional data, are becoming increasingly available in various fields, and examples can be found in neuroimaging analysis where various brain regions of interest (ROIs) are scanned over time for individuals.

A typical example is the electroencephalography (EEG) data (Qiao et al., 2019), the detailed description of this dataset is provided in Section 5. One focus of interest is to classify different groups using brain signals. A straightforward way is to perform p individual FPCAs and apply high-dimensional techniques to reduced variables. Nevertheless, this strategy has some drawbacks. First, it is computationally expensive since p univariate FPCAs and additional high-dimensional methods are required. Second, one of the advantages of FPCA is to provide a parsimonious representation of data, while separate decompositions fail to model the correlation between processes and make the interpretation difficult. Moreover, the correlation among FPC scores from different processes may lead to multicollinearity in subsequent regression analysis (e.g., Müller and Yao, 2008). Finally, there is no theoretical guarantee for collectively treating high-dimensional functional features, nor for the performance of subsequent analysis. Therefore, classical methods and results are no longer applicable, which motivates the study of scalable FPCA in high dimensions.

Recently there has been elevated interest in studying multivariate FPCA. A standard approach is to concatenate the multiple functions to perform univariate FPCA (Ramsay and Silverman, 2005). Berrendero et al. (2011) performed a classical multivariate PCA for each value of the domain on which the functions are observed. Chiou et al. (2014) proposed a

normalized version of multivariate FPCA. Jacques and Preda (2014) introduced a method based on basis expansions, and Happ and Greven (2018) extended it to handle multivariate functional data observed on different (dimensional) domains. In the aforementioned works, the number of functional variables p is considered finite and much smaller than the sample size n . As a consequence, these methods fail to deal with functional data in high dimensions due to both computational and theoretical issues.

Likewise in multivariate statistics, the sample eigenvectors are inconsistent in high dimensions (Johnstone and Lu, 2009). A typical strategy is to impose the sparsity assumption on eigenvectors or principal subspace (Zou et al., 2006; Shen and Huang, 2008; Vu and Lei, 2013, among others). In particular, Johnstone and Lu (2009) proposed an estimator based on diagonal thresholding that screens out variables with small sample variances. In spite of extensive literature for sparse PCA, the extension to high-dimensional functional processes is still challenging, as the functional data are usually observed at grids with noise and the large p leads to error accumulation. Moreover, there is no available notion of sparsity in the context of high-dimensional functional data where not only is p large, but also each variable is an intrinsically infinite-dimensional process.

Our goal is to establish an accountable yet parsimonious sparse FPCA for high-dimensional functional data. We begin with establishing the connection between the multivariate K-L expansion and univariate orthonormal basis representation for infinite-dimensional processes, which is a generalization of Happ and Greven (2018) assuming that each process has a finite-dimensional representation. The established relationship is flexible to allow any suitable basis expansions such as B-spline basis and Wavelet basis. Based on this relationship, our method avoids performing univariate FPCAs which are computationally expensive and introduce data-dependent uncertainty in high dimensions. The main contributions include coupling the sparsity concept in multivariate statistics with functional variables and providing two sensible sparsity regimes necessary for high-dimensional functional data, namely the l_0 and weak l_q sparsity. While these sparsity notions are standard in multivariate statistics,

there has been no attempt to generalize them to functional settings. The sparsity structure motivates us to adopt the thresholding technique which can identify important processes. The proposed algorithm is easy to compute without performing smoothing. Moreover, we carefully investigate the theoretical properties of resulting estimators, as well as the complex interaction between the eigen problem and the sparsity regularization. A phase transition phenomenon intrinsic to discretely observed functional data in terms of the sampling rate is revealed in this context. To our knowledge, this has not been discussed in literature and provides insight into consistent dimension reduction for discretely observed noisy functional data in high dimensions.

The remainder of the article is organized as follows. In Section 2, we provide two sparsity regimes and introduce the proposed approach sparse FPCA (sFPCA). In Section 3, we present theoretical results for sFPCA under the sparsity regimes. Simulation results for both trajectory recovery and subsequent classification for comparison are included in Section 4, followed by an application to the EEG data in Section 5. More theoretical results and technical proofs are deferred to the Supplementary Material.

2. SPARSE FPCA IN HIGH DIMENSIONS

2.1 Multivariate Karhunen-Loève expansion

Suppose that the functional data are $\mathbf{X} = (X_1, \dots, X_p)^T$ and each $X_j(\cdot) \in L^2(\mathcal{T})$ is a square-integrable random function defined on a compact interval $\mathcal{T} = [0, 1]$ with continuous mean and covariance functions. Let \mathbb{H} denote a Hilbert space of p -dimensional vectors of functions in $L^2(\mathcal{T})$, equipped with the inner product $\langle \mathbf{f}, \mathbf{g} \rangle_{\mathbb{H}} = \sum_{j=1}^p \langle f_j, g_j \rangle = \sum_{j=1}^p \int_{\mathcal{T}} f_j(t)g_j(t)dt$ and the norm $\|\cdot\|_{\mathbb{H}} = \langle \cdot, \cdot \rangle_{\mathbb{H}}^{1/2}$. Without loss of generality (w.l.o.g.), we assume that all processes are centered, i.e., $E\{X_j(t)\} = 0$. Define the covariance function $G(s, t) = E\{\mathbf{X}(s)\mathbf{X}(t)^T\} = \{G_{jk}(s, t)\} \in \mathbb{R}^{p \times p}$.

According to the multivariate Mercer's theorem, there exists a complete orthonormal basis $\{\boldsymbol{\psi}_k : k \geq 1\}$ and the corresponding sequence of eigenvalues $\{\lambda_k > 0 : k \geq 1\}$ such that

$G(s, t)$ has the representation $G(s, t) = \sum_{k=1}^{\infty} \lambda_k \boldsymbol{\psi}_k(s) \boldsymbol{\psi}_k(t)^T$, where $\langle \boldsymbol{\psi}_{k_1}, \boldsymbol{\psi}_{k_2} \rangle_{\mathbb{H}} = \delta_{k_1 k_2}$, where $\delta_{k_1 k_2}$ is 1 if $k_1 = k_2$ and 0 otherwise, and $\lambda_1 \geq \lambda_2 \geq \dots \geq 0$. Accordingly, the multivariate K-L expansion is $\mathbf{X}(t) = \sum_{k=1}^{\infty} \eta_k \boldsymbol{\psi}_k(t)$, where $\boldsymbol{\psi}_k(t) = (\psi_{k1}, \dots, \psi_{kp})^T$ and the scores $\eta_k = \langle \mathbf{X}, \boldsymbol{\psi}_k \rangle_{\mathbb{H}}$ are random variables with mean zero and variances $E(\eta_k^2) = \lambda_k$. It leads to a single set of scores for each subject, which serves as a proxy of multivariate functional data. In contrast, the univariate Karhunen-Loève expansion is $X_j(t) = \sum_{k=1}^{\infty} \xi_{jk} \phi_{jk}(t)$, where $\xi_{jk} = \langle X_j, \phi_{jk} \rangle$ and $\phi_{jk}(t)$ are eigenfunctions satisfying $\langle \phi_{jk_1}, \phi_{jk_2} \rangle = \delta_{k_1 k_2}$. To avoid the ambiguity, we refer to $\boldsymbol{\psi}_k$ and ϕ_{jk} as multivariate and univariate eigenfunctions, respectively. Clearly the main difference between these two expansions is that the $\boldsymbol{\psi}_k(\cdot)$ are vector-valued while the scores η_k are scalars, which allows a parsimonious representation of data and the same structure for each subject. Our focus of interest is to establish consistent estimators for $\boldsymbol{\psi}_k$, and as a consequence, the scores η_k and parsimonious data recovery are obtained.

2.2 Basis representation for Karhunen-Loève expansion

In high dimensions, computational tractability is one of practical considerations. Either pre-smoothing (Ramsay and Silverman, 2005) or post-smoothing (Yao et al., 2005a) method for FPCA is computationally prohibitive when p is large. A remedy is to represent functional processes via a set of orthonormal basis, consequently, the covariance/eigenfunctions are expressed and estimated accordingly (Rice and Wu, 2000; James et al., 2001). We derive the relationship between univariate basis expansions and multivariate K-L representations in Proposition 1 for intrinsically infinite-dimensional processes, setting stage for the proposed methodology.

Proposition 1. *Assume that $\mathbf{X} \in \mathbb{H}$. Given the univariate orthonormal basis representation for each random process $X_j = \sum_{l=1}^{\infty} \theta_{jl} b_l$, denote $u_{kjl} = \int_{\mathcal{T}} b_l(t) \psi_{kj}(t) dt$, then we have the equation*

$$\sum_{j'=1}^p \sum_{l'=1}^{\infty} \text{cov}(\theta_{jl}, \theta_{j'l'}) u_{kj'l'} = \lambda_k u_{kjl}, j = 1, \dots, p, k, l = 1, 2, \dots, \quad (1)$$

where $\boldsymbol{\psi}_k$ and λ_k are eigenfunctions and corresponding eigenvalues of the covariance operator of \mathbf{X} . The eigenfunctions $\boldsymbol{\psi}_k$ and the scores η_k are

$$\psi_{kj}(t) = \sum_{l=1}^{\infty} u_{kjl} b_l(t), \quad \eta_k = \sum_{j=1}^p \sum_{l=1}^{\infty} u_{kjl} \theta_{jl}, \quad j = 1, \dots, p, k = 1, 2, \dots$$

By contrast, Happ and Greven (2018) gave a similar relationship under the assumption of finite-dimensional representations. Proposition 1 is a generalization in line with the intrinsically infinite-dimensional nature of functional data. Accordingly, the j th component of eigenfunctions $\boldsymbol{\psi}_k$ can be expressed as a linear combination of bases $\{b_l : l \geq 1\}$ with generalized Fourier coefficients $\{u_{kjl} : l \geq 1\}$ obtained from (1) and that the scores η_k are linear combinations of basis coefficients $\{\theta_{jl} : j = 1, \dots, p; l = 1, \dots, \infty\}$.

Proposition 1 allows arbitrary basis expansions incorporating a set of pre-fixed basis (e.g., B-splines, wavelets) or data-driven basis (i.e., eigenfunctions). Although eigenfunctions can be estimated from data, it is inadvisable to employ univariate FPCA which is computationally prohibitive for large p and introduce data-dependent uncertainty. Therefore, we adopt pre-fixed basis functions to represent the trajectories and covariance/eigenfunctions (Rice and Wu, 2000; James et al., 2001). W.l.o.g., we use a common complete and orthonormal basis $\{b_l : l \geq 1\}$ in $L^2(\mathcal{T})$ for p processes and do not pursue other complicated basis-seeking procedures that are peripheral to the key proposal. Let the underlying random functions be expressed as $x_{ij} = \sum_{l=1}^{\infty} \theta_{ijl} b_l$, where the coefficients $\theta_{ijl} = \int_{\mathcal{T}} x_{ij}(t) b_l(t) dt$ are random variables with mean zero and variances $E(\theta_{ijl}^2) = \sigma_{jl}^2$, and we refer to the total variability of the j th process as its energy denoted by $V_j = \sum_{l=1}^{\infty} \sigma_{jl}^2 < \infty$. It is necessary to regularize infinite-dimensional processes, and a natural means is truncation that serves as a sieve-type approximation. The size of truncation may diverge with the sample size n , which maintains the nonparametric nature of the proposed method. Denote the number of basis functions by s_{nj} , also referred to as the truncation parameter of the j th process when no confusion arises, $j = 1, \dots, p$. It suffices to use a common s_n for the method development and theoretical analysis, assuming $s_{nj} \asymp s_n$, where $a_n \asymp b_n$ if $0 < \liminf_{n \rightarrow \infty} a_n/b_n \leq \limsup_{n \rightarrow \infty} a_n/b_n < \infty$.

Through Proposition 1, the multivariate FPCA can be transformed into performing the

classical PCA on the covariance matrix of all basis coefficients. Moreover, this motivates an easy-to-implement estimation procedure under sensible sparsity regimes described in Section 2.3.

Remark 1. Pre-fixed basis expansion is a fairly popular method to deal with functional data, see James et al. (2001), Ramsay and Silverman (2005) and Koudstaal and Yao (2018), among others. Although the Proposition 1 is presented using the same set of orthonormal basis functions for p random processes to simplify the exposition, our method is directly applicable for allowing arbitrary and different bases for different processes. The proof of the more general form is presented in the Supplementary Material. Such generality in some sense guarantees that our method is capable of modeling functions with striking local features by choosing suitable basis such as wavelet that possesses spatial adaptation (Donoho and Johnstone, 1994).

2.3 Sparsity regimes

To our knowledge, there is no available notion of sparsity in the context of FPCA for high-dimensional cases where p is large, though the sparsity of principal eigenvectors or subspace (Vu and Lei, 2013) in multivariate statistics is well defined. The formulation of sparsity in our problem is nontrivial. First, FPCA depends on vector-valued eigenfunctions, not vectors anymore. Second, functional data are usually discretely observed with error, which leads to more challenging estimation and data recovery due to error accumulation in high dimensions. Therefore, we wish to reduce the dimensionality from p to a much smaller one. To succeed, the total energy of data should be concentrated in a smaller number of processes. To achieve this, we need additional structures for high-dimensional functional data.

For the moment, we first review a typical decay assumption for univariate functional data (Koudstaal and Yao, 2018). Recall that $\sigma_{jl}^2 = E(\theta_{ijl}^2)$ where θ_{ijl} is the basis coefficient of x_{ij} . Assume for adequately large s_n ,

$$\sigma_{j(l)}^2 = O\{l^{-(1+2\alpha)}\}, \quad l \leq s_n,$$

$$\sigma_{jl}^2 = O\{l^{-(1+2\alpha)}\}, \quad l > s_n, \quad (2)$$

uniformly in $j = 1, \dots, p$, where $\alpha > 0$ and $\sigma_{j(l)}^2$ denote the ordered values such that $\sigma_{j(1)}^2 \geq \sigma_{j(2)}^2 \geq \dots$. This assumption ensures that the bulk of signals in each process are contained in the largest s_n coordinates. We stress that the location and the order of coordinates are *unknown* for spatial adaptation (Donoho and Johnstone, 1994), which is also realistic for pre-specified basis.

Remark 2. The decay in (2) is applied to ordered variances (up to s_n), where the ordering and location are unknown. When projecting each process onto the corresponding univariate eigenfunctions $\phi_{jl}(t)$, the variances of coefficients σ_{jl}^2 are non-increasingly ordered eigenvalues. In this way, the decay condition (2) holds under very general assumptions, e.g., the covariance function $G_{jj}(s, t)$ satisfying the Sacks-Ylvisacker conditions of order $r = \alpha - \frac{1}{2} \geq 0$ (Ritter et al., 1995). When employing general bases, it is also reasonable to expect that the decay in (2) is satisfied if suitable bases are chosen for the underlying processes. Readers can refer to Koudstaal and Yao (2018) for more discussion on this issue.

The decay condition (2) is not enough to handle high-dimensional settings since it does not provide any regularization for the high dimensionality p . Recall that $\mathbf{V} = (V_1, \dots, V_p)^T$ and $V_j = \sum_{l=1}^{\infty} \sigma_{jl}^2$ is the total energy of the j th process. In the following, two types of sparsity l_0 and weak l_q are assumed for the high-dimensional vector \mathbf{V} , which is shown to be reasonable in practice as illustrated in Section 5.

l_0 sparsity. We consider the case where only a small fraction of processes contain signals and the rest do not. Here the l_0 sparsity is in the sense of $\|\mathbf{V}\|_0 = g \ll p$. It is assumed w.l.o.g. that the first g processes contain signals with comparable energies and $V_j \equiv 0$, for $j = g + 1, \dots, p$. Moreover, the variances of coefficients for these g processes satisfy (2).

Weak l_q sparsity. Another typical situation of interest is to incorporate processes with small energies that decay in a nonparametric manner. To be specific, assume that for some positive constant $C > 0$,

$$V_{(j)} \leq Cj^{-2/q}, \quad j = 1, \dots, p, \quad (3)$$

where $0 < q < 2$ determines the sparsity level, i.e., smaller q entails sparser processes. Consequently, the total energy is concentrated in the leading processes with large energies. Thus, a reasonable assumption is

$$\begin{aligned}\sigma_{(j)(l)}^2 &= O\{j^{-2/q}l^{-(1+2\alpha)}\}, \quad l \leq s_n, \\ \sigma_{(j)l}^2 &= O\{j^{-2/q}l^{-(1+2\alpha)}\}, \quad l > s_n,\end{aligned}\tag{4}$$

where $\sigma_{(j)(l)}^2$ is the l th largest variance of coefficients for the process with energy $V_{(j)}$, and the extra term $j^{-2/q}$ in comparison with (2) is due to the sparsity assumed in (3).

To summarize, different from the multivariate case, both the functional l_0 and weak l_q sparsity contain two types of decay: within processes determined by α , and between processes determined by q . The decay within processes means that the variances of coefficients exhibit certain sparsity, while the decay between processes depicts the sparsity assumption on the high-dimensional energy vector \mathbf{V} . The within-process sparsity is standard for univariate functional data (Koudstaal and Yao, 2018), while the between-process sparsity is for the first time specified to regularize the high dimensionality p in the context of functional data.

2.4 Proposed threshold estimation and recovery

Distinguishing from existing works, we aim to model eigenfunctions of p random processes where $p \gg n$. The standard FPCA is no longer applicable due to computational and theoretical issues including the proposal by Happ and Greven (2018), as illustrated in Sections 4 and 5. In this section, we propose a unified framework to perform sparse FPCA based on the relationship declared in Proposition 1.

Let $\{\mathbf{x}_i : i = 1, \dots, n\}$ be independent and identically distributed (i.i.d.) realizations from \mathbf{X} , where $\mathbf{x}_i = (x_{i1}, \dots, x_{ip})^\top$. In reality, we do not observe the entire trajectories x_{ij} but some noisy measurements, $y_{ijk} = x_{ij}(t_k) + \epsilon_{ijk}$, $t_k \in \mathcal{T}$, where ϵ_{ijk} is measurement error independent of x_{ij} with mean zero and variance σ^2 , $i = 1, \dots, n, j = 1, \dots, p, k = 1, \dots, m$. For the sake of simplifying statements, we assume that the grid is regular, i.e., $t_k = k/m$, while our methodology can be directly applied to more general grid structures. The extremely

sparse case when only a few measurements are available for each trajectory (Yao et al., 2005a) is beyond the scope of this article which can be investigated for future study.

According to the Proposition 1, we first perform basis expansions for all processes based on discrete observations. Let $I_k = ((k-1)/m, k/m]$, $k = 2, \dots, m$ and $I_1 = [0, 1/m]$, we define $y'_{ij}(t) = y_{ijk}$ for $t \in I_k$, and define x'_{ij} , ϵ'_{ij} similarly. Observe that $y'_{ij} = x'_{ij} + \epsilon'_{ij}$, and projecting y'_{ij} onto the orthonormal basis $b_l(t)$ yields $\hat{\theta}_{ijl} = \tilde{\theta}_{ijl} + \tilde{\epsilon}_{ijl}$, $l = 1, \dots, s_n$, for a suitable choice of s_n , where $\hat{\theta}_{ijl} = \int_0^1 y'_{ij}(t)b_l(t)dt$ are estimated basis coefficients and $\tilde{\epsilon}_{ijl}$ is independent of $\tilde{\theta}_{ijl}$ with mean zero and variance $\tilde{\sigma}^2 = E(\tilde{\epsilon}_{ijl}^2) = \sigma^2 m^{-1} + O(m^{-2})$ due to discretization. We emphasize that our method does not demand smoothing discretely observed noisy data, which facilitates computation considerably. The impact of noise/discretization on resulting estimators is theoretically analyzed in Section 3.

Assume that θ_{ijl} and ϵ_{ijk} are jointly Gaussian. Therefore, we conclude that $\hat{\sigma}_{jl}^2 \sim (\sigma^2 m^{-1} + \tilde{\sigma}_{jl}^2) \chi_n^2/n$ where $\hat{\sigma}_{jl}^2 = n^{-1} \sum_{i=1}^n \hat{\theta}_{ijl}^2$ and $\tilde{\sigma}_{jl}^2 = E(\tilde{\theta}_{ijl}^2)$. For the method development, it suffices to use σ^2/m as an approximation of $\tilde{\sigma}^2$ to construct our estimators. The difference between $\tilde{\sigma}_{jl}^2$ and σ_{jl}^2 is negligible for large m , and large values of σ_{jl}^2 are prone to have large sample variances $\hat{\sigma}_{jl}^2$. The idea is to include only the variables with largest sample variances. Thus, we perform the coordinate selection as follows,

$$\hat{I} = \{(j, l), j = 1, \dots, p; l = 1, \dots, s_n : \hat{\sigma}_{jl}^2 \geq m^{-1} \sigma^2 (1 + \alpha_n)\}, \quad (5)$$

where $\alpha_n = \alpha_0 \{n^{-1} \log(ps_n)\}^{1/2}$, $\alpha_0 > \sqrt{12}$ is a suitable positive constant for theoretical guarantees (Johnstone and Lu, 2009). The choice of α_n is based on the concentration result of basis coefficients, and the number of basis s_n comes from the sieve-like truncation for functional processes. When $l > m^{1/(2\alpha+1)}$ or $j > m^{q/2}$ the signals decrease rapidly below the noise level. We expect that the proposed strategy retains only sizable signals and forces the rest to zero leading to the desired model parsimony.

Remark 3. Let $\hat{\psi}_k$ be the multivariate eigenfunctions of $\hat{\mathbf{X}}$. Note that,

$$\|\psi_k - \hat{\psi}_k\|_{\mathbb{H}}^2 \leq C \frac{\{E(\|\hat{\mathbf{X}}\|_{\mathbb{H}}^2) + E(\|\mathbf{X}\|_{\mathbb{H}}^2)\} E(\|\hat{\mathbf{X}} - \mathbf{X}\|_{\mathbb{H}}^2)}{(\lambda_k - \lambda_{k+1})^2},$$

for some $C > 0$, which is shown in the Supplementary Material. Using Parseval's identity and the orthonormality of the basis functions, the error $E\|\hat{\mathbf{X}} - \mathbf{X}\|_{\mathbb{H}}^2$ is expressed in terms of $\sum_j \sum_l E(\hat{\theta}_{jl} - \theta_{jl})^2$. Intuitively, when σ_{jl}^2 is small, the signal is mostly obscured by the noise and may be discarded.

Denote the retained coefficients by $\boldsymbol{\theta}_j = (\theta_{jl}, (j, l) \in \hat{I})^T$. Let $S_{\hat{I}} = n^{-1} \sum_{i=1}^n \hat{\boldsymbol{\theta}}_{i\hat{I}} \hat{\boldsymbol{\theta}}_{i\hat{I}}^T$ be the sample covariance matrix. Based on Proposition 1, we perform multivariate PCA on $S_{\hat{I}}$ to yield principal eigenvectors $\hat{\mathbf{u}}_k, k = 1, \dots, r_n$. Finally, we transform the results back to functional spaces,

$$\hat{\psi}_{kj}(t) = \sum_{l:(j,l) \in \hat{I}} \hat{u}_{kjl} b_l(t), \quad \hat{\eta}_{ik} = \sum_{(j,l):(j,l) \in \hat{I}} \hat{u}_{kjl} \hat{\theta}_{ijl}, \quad \hat{\mathbf{x}}_i^{r_n} = \sum_{k=1}^{r_n} \hat{\eta}_{ik} \hat{\boldsymbol{\psi}}_k.$$

for $j = 1, \dots, p, k = 1, \dots, r_n$. Let N_j be the number of retained coefficients for the j th process. Apparently, $N_j = 0$ implies that elements of the j th block of $\hat{\boldsymbol{\theta}}$ satisfy $\hat{\theta}_{jl} \notin \hat{\boldsymbol{\theta}}_j$ for all $l = 1, \dots, s_n$, then each element of the j th block of $\hat{\mathbf{u}}_k$ equals to zero, $\hat{\psi}_{kj}(t) \equiv 0, k = 1, \dots, r_n$, i.e., the j th random process will be ruled out. Otherwise for $N_j > 0$, there exists at least one element of j th block of $\hat{\boldsymbol{\theta}}$ satisfying $\hat{\theta}_{jl} \in \hat{\boldsymbol{\theta}}_j$, then the j th random process will be retained. The implementation algorithm is summarized below.

Remark 4. In practice, the variance $m^{-1}\sigma^2$ is usually unknown, we replace it by a quantile estimator $Q_{\rho}(\hat{\sigma}_{jl}^2 : j = 1, \dots, p, l = 1, \dots, s_n)$ as suggested by Koudstaal and Yao (2018), where $Q_{\rho}(\mathbf{z}), 0 < \rho < 1$, is the 100ρ th sample quantile of sorted values in a vector \mathbf{z} . We also propose an objective-driven method to choose the parameter ρ which controls the desired sparsity level, the truncation s_n and the number of principal components r_n . For unsupervised problems, ρ may be determined by a trade-off between the quality of recovery and model complexity, i.e., the number of retained processes, while we use K -fold cross-validation to choose s_n and the fraction of variance explained to choose r_n for reduced computation. If one considers a supervised problem, such as regression or classification, parameters ρ, s_n and r_n may be tuned by K -fold cross-validation to minimize the prediction/classification error. From our theoretical analysis and numerical experience, as a practical guidance, one may

Algorithm 1 The algorithm for sFPCA.

Generally, denote $\bar{y}_j = n^{-1} \sum_{i=1}^n y'_{ij}$ and $\tilde{y}_{ij} = y'_{ij} - \bar{y}_j$.

(i) *Projection and truncation.* Project \tilde{y}_{ij} onto the orthonormal basis functions $b_l(t)$ to yield

$$\hat{\theta}_{ijl} = \int_0^1 \tilde{y}_{ij}(t) b_l(t) dt, j = 1, \dots, p, l = 1, \dots, s_n.$$

(ii) *Thresholding.* Calculate the sample variances $\hat{\sigma}_{jl}^2$ of $\hat{\theta}_{ijl}$ and perform the subset selection based on the rule,

$$\hat{I} = \{(j, l), j = 1, \dots, p; l = 1, \dots, s_n : \hat{\sigma}_{jl}^2 \geq m^{-1} \sigma^2 (1 + \alpha_n)\},$$

where $\alpha_n = 4\{n^{-1} \log(ps_n)\}^{1/2}$ in our numerical studies.

(iii) *Eigen-decomposition and transformation.* Calculate the sample covariance matrix $S_{\hat{I}}$ of retained coefficients $\hat{\theta}_{\hat{I}}$. Perform PCA on $S_{\hat{I}}$ to yield principal eigenvectors $\hat{\mathbf{u}}_k, k = 1, \dots, r_n$, then calculate

$$\hat{\psi}_{kj}(t) = \sum_{l:(j,l) \in \hat{I}} \hat{u}_{kjl} b_l(t), \quad \hat{\eta}_{ik} = \sum_{(j,l):(j,l) \in \hat{I}} \hat{u}_{kjl} \hat{\theta}_{ijl}, \quad \hat{\mathbf{x}}_i^{r_n} = \bar{\mathbf{y}} + \sum_{k=1}^{r_n} \hat{\eta}_{ik} \hat{\psi}_k,$$

where $\bar{\mathbf{y}} = (\bar{y}_1, \dots, \bar{y}_p)^T$.

choose an adequate s_n to characterize the features and mainly focus on choices of ρ and r_n . More details and empirical evidence are offered in Section 4.

Remark 5. To illustrate the computational advantage of our algorithm, we examine the order of computation complexity for estimation of covariance and eigenstructure, in contrast to that of HG method (Happ and Greven, 2018) and p univariate FPCAs. The HG method operates with $O(np^2 s_n^2 + p^3 s_n^3)$ complexity, which scales poorly for high-dimensional functional data. The univariate FPCA with either presmoothing (Ramsay and Silverman, 2005) or post-smoothing (Yao et al., 2005a) requires computation of order $O(npm^2 + pm^3)$ that is fairly intensive for densely observed high-dimensional functional data. Our method retains at most $N = \sum_{j=1}^p N_j$ non-zero coordinates, where $N \ll ps_n$ almost surely according to Lemma 1. Thus, our procedure operates with the complexity at the order of $O(nps_n + nN^2 + N^3)$, which

achieves considerable computational savings and is demonstrated in the numerical studies in Sections 4 and 5.

We stress that the analysis of functional data are more challenging than that of multivariate data in high dimensions. First, since functional data are recorded at a grid of points, the estimation error from observed discrete version to functional continuous version needs to be investigated with care. Second, most literature assumed spiked covariance model for sparse PCA, while it is not valid for functional data that has potentially infinite rank. Third, as discussed in Section 2.3, the variances of coefficients involve two types of decay: within processes, i.e., α , and between processes, i.e., q .

3. THEORETICAL PROPERTIES

In this section, we mainly focus on the consistency of the eigenfunction estimates under the weak l_q sparsity for space economy, and more results for the l_0 sparsity and trajectory recovery are presented in the Supplementary Material. We state several basic conditions here and more conditions concerning properties of underlying processes and the sampling schemes are provided in the Supplementary Material. Condition 1 is standard for functional data (Hall and Horowitz, 2007), and prevents the spacing between adjacent eigenvalues from being too small and implies that $\lambda_k \geq Ck^{-a}$.

Condition 1. For $a > 1$ and $C > 0$, $\lambda_k - \lambda_{k+1} \geq Ck^{-a-1}$, $k \geq 1$.

Condition 2. $p = O\{\exp(n^\beta)\}$ for $0 < \beta < 1$.

The number of functional processes p is allowed to be ultrahigh. Regarding the sampling frequency m , it should be large enough to control the discretization error such that $\tilde{\sigma}_{jl}^2/\sigma_{jl}^2 \rightarrow 1$. Under Condition 3, the thresholding value in (5) is determined using concentration inequalities.

Condition 3. The sampling rate satisfies $m = O(n^\gamma)$ for $\gamma > (1 - \beta)/2$.

The Condition 3 is milder than that imposed by Kong et al. (2016). We shall see from later theorems that this assumption on sampling rate plays an indispensable role in approximation/estimation error.

In the asymptotic analysis, we consider the approximation error caused by truncation/thresholding as well as the statistical estimation error. For the eigenfunctions, one has the following decomposition: $\|\boldsymbol{\psi}_k - \hat{\boldsymbol{\psi}}_k\|_{\mathbb{H}} \leq \|\boldsymbol{\psi}_k - \tilde{\boldsymbol{\psi}}_k\|_{\mathbb{H}} + \|\tilde{\boldsymbol{\psi}}_k - \hat{\boldsymbol{\psi}}_k\|_{\mathbb{H}}$, where $\tilde{\boldsymbol{\psi}}_k$ are the eigenfunctions of thresholded processes $\tilde{\mathbf{X}}$ with $\tilde{X}_j = \sum_{l:(j,l) \in \hat{I}} \theta_{jl} b_l$. The first term on the right-hand side could be viewed as the approximation error, while the second term is interpreted as the estimation error. Recall that N_j is the number of retained coefficients for X_j . We mention that the approximation error here is also random because it depends on random quantities N_j determined by thresholding. Let g_n denote the number of retained processes that may grow with the sample size n in a nonparametric manner. Recall that V_j are the energies of processes. W.l.o.g., we assume for the moment that $V_1 \geq \dots \geq V_p$. The following lemma quantifies g_n and the number of retained coefficients N_j . One challenge is to deal with the discretization error with care when applying the concentration results.

Lemma 1. *Under Conditions 2-3, S1-S4 in the Supplementary Material and the weak l_q sparsity, the number of retained coefficients for X_j satisfies $N_j \leq C\{m^{-1}\sqrt{\log p/n}\}^{-1/(2\alpha+1)}j^{-2/\{q(2\alpha+1)\}}$ and the number of retained processes $g_n \leq C\{m^{-1}\sqrt{\log p/n}\}^{-q/2}$ almost surely (a.s.) for some $C > 0$.*

Lemma 1 illustrates that many processes with small energies will be excluded from the estimation. The term $j^{-2/\{q(2\alpha+1)\}}$ indicates that the quantity N_j will decrease as V_j decays. Apparently, the processes will be screened out if V_j decays to a smaller magnitude, i.e., N_j will be zero for those processes. The retained coefficients of X_j are thresholded from total s_n terms, which to some extent implies a sufficiently large s_n .

Theorem 1 (Approximation Error). *Under the weak l_q sparsity (4), if Conditions 1-3 and S1-S4, S6 in the Supplementary Material hold and $\langle \boldsymbol{\psi}_k, \tilde{\boldsymbol{\psi}}_k \rangle_{\mathbb{H}} \geq 0$, then uniformly for $k = 1, \dots, r_n$, we have the following.*

Case 1. When $q(2\alpha + 1) > 2$,

$$\|\tilde{\boldsymbol{\psi}}_k - \boldsymbol{\psi}_k\|_{\mathbb{H}} = O(k^{a+1}g_n^{1/2-1/q}), \quad a.s.,$$

Case 2. When $q(2\alpha + 1) = 2$,

$$\|\tilde{\boldsymbol{\psi}}_k - \boldsymbol{\psi}_k\|_{\mathbb{H}} = O \left[k^{a+1} \{m^{-1} \sqrt{\log p/n}\}^{\alpha/(2\alpha+1)} (\log g_n)^{1/2} \right], \quad a.s.,$$

Case 3. When $q(2\alpha + 1) < 2$,

$$\|\tilde{\boldsymbol{\psi}}_k - \boldsymbol{\psi}_k\|_{\mathbb{H}} = O \left[k^{a+1} \{m^{-1} \sqrt{\log p/n}\}^{\alpha/(2\alpha+1)} \right], \quad a.s..$$

Theorem 1 establishes rates of convergence for approximation error based on the comparison of α and q which represent sparsity levels within and between processes, respectively. The term k^{a+1} is attributed to the increasing error of approximating higher order eigenelements $\boldsymbol{\psi}_k$. The approximation error is decomposed into two terms which incorporate errors caused by screening out processes with small energies and excluding coefficients with small variances for the retained processes. Observe that smaller q and larger α lead to sparser settings. When α is relatively large, saying $\alpha > 1/q - 1/2$ as in Case 1, the energies of processes V_j do not decay so fast that the term $g_n^{1/2-1/q}$ caused by excluding the processes with small energies dominates. Intuitively in this case, the processes are more like scalar variables since the between-process sparsity dominates. When q is relatively small, the rates are determined by the term $\{m^{-1} \sqrt{\log p/n}\}^{\alpha/(2\alpha+1)}$ attributed to thresholding coefficients of the retained processes, and the additional term $\log g_n$ in Case 2 is due to the fact that the N_j corresponds to $j^{-2/\{q(2\alpha+1)\}}$ as a consequence of the decaying energies.

Theorem 2 (Estimation Error). *Under the weak l_q sparsity (4), if Conditions 1-3, S1-S5, S7 in the Supplementary Material hold and $\langle \hat{\boldsymbol{\psi}}_k, \tilde{\boldsymbol{\psi}}_k \rangle_{\mathbb{H}} \geq 0$, then uniformly for $k = 1, \dots, r_n$, we have the following.*

Case 1. When $\gamma > 1/(2 - q)$,

$$\|\tilde{\boldsymbol{\psi}}_k - \hat{\boldsymbol{\psi}}_k\|_{\mathbb{H}} = O_p(kn^{-1/2}),$$

Case 2. When $(1 - \beta)/2 < \gamma \leq 1/(2 - q)$ with $\log p/n = O(n^{\beta-1})$,

$$\|\tilde{\boldsymbol{\psi}}_k - \hat{\boldsymbol{\psi}}_k\|_{\mathbb{H}} = O_p(k^{a+1}g_n^{1/2}m^{-1}).$$

The estimation error does not involve the term N_j , as we quantify the discretization error of retained coefficients via retained processes using Bessel's inequality. The corresponding rate of convergence for the covariance of retained processes is of the order $O_p(n^{-1/2} + g_n^{1/2}m^{-1})$, where g_n is the number of retained processes determined by quantities q and γ from Lemma 1. Cases 1 and 2 correspond to the parametric covariance estimation error and discretization error, respectively. The rates of convergence exhibit a phase transition phenomenon depending on the sampling rate γ . When the data are sufficiently dense as in Case 1, the error term for covariance estimation induced by the discretization is negligible, achieving the parametric rate $n^{-1/2}$ as if the whole functions were observed. Using similar techniques in Hall and Horowitz (2007), we obtain a sharp bound for eigenfunctions. Otherwise as in Case 2, slower convergence rates for eigenfunctions by Theorem 1 in Hall and Hosseini-Nasab (2006) are attained by taking the discretization error m^{-1} into account.

Combining the approximation error and estimation error, one can see that the convergence rate of $\|\hat{\boldsymbol{\psi}}_k - \boldsymbol{\psi}_k\|_{\mathbb{H}}$ can not exceed the parametric rate which is consistent with the common sense. The phase transition caused by smoothing has been discussed in Cai and Yuan (2011, 2010) and Zhang and Wang (2016) for univariate functional data, while it is revealed for the first time for high-dimensional functional data.

Under the l_0 sparsity and some regularity conditions in the Supplementary Material, if $\min_{j \in \{1, \dots, g\}} \max_l \sigma_{jl}^2 \gg m^{-1} \sqrt{\log p/n}$, then our method successfully selects g significant processes almost surely as $n \rightarrow \infty$. The approximation and estimation errors under the l_0 sparsity can be analyzed in a similar manner. For the approximation error, it is caused by the thresholding step where coefficients with small variances are excluded. The estimation error exhibits phase transition phenomenon at $\gamma = 1/2$. Detailed results are provided in the Supplementary Material.

4. SIMULATION STUDIES

4.1 Sparse FPCA

To illustrate the performance of the proposed method for high-dimensional functional variables, we designate two sparsity settings as discussed in Section 2.3. We first examine the performance in an unsupervised fashion.

The noisy observations are generated from $y_{ij}(t_k) = x_{ij}(t_k) + \epsilon_{ijk} = \sum_{l=1}^s \theta_{ijl} \phi_l(t_k) + \epsilon_{ijk}$, $t_k \in [0, 1]$, $j = 1, \dots, p$, where ϵ_{ijk} are i.i.d. from $N(0, 1)$. Let $\phi_l(t)$ be functions in the Fourier basis, $\phi_l(t) = \sqrt{2} \sin\{\pi(l+1)t\}$ when l is odd, $\phi_l(t) = \sqrt{2} \cos(\pi lt)$ when l is even. We set $s = 50$ to mimic the infinite nature of functional data. The equally spaced grids are $\{t_k\}_{k=1}^m = \{0, 0.01, \dots, 1\}$ with $m = 101$, and the sample size $n = 100$. Each simulation consists of 100 Monte Carlo runs.

Processes under the l_0 sparsity. Let $p = 50, 100, 200$ and the number of processes containing signals $g = 2, 10$, respectively. The underlying true signals $x_{ij}(t_{ijk}) = \sum_{l=1}^s \theta_{ijl} \phi_l(t_{ijk})$ for $j = 1, \dots, g$, and the rest $x_{ij}(t_{ijk}) = 0$. Denote $\boldsymbol{\theta} = (\theta_{11}, \dots, \theta_{1s}, \dots, \theta_{g1}, \dots, \theta_{gs})^\top$. The coefficients $\boldsymbol{\theta}_i$ are generated from $N(\mathbf{0}, C)$, where $C = VD V^\top$ with an orthonormal matrix V and a diagonal matrix with diagonal entries $D_{\nu\nu} = 16\nu^{-7/3}$, $\nu = 1, \dots, gs$. The dependence between coefficients leads to correlated processes.

Processes under the weak l_q sparsity. To generate $x_{ij}(\cdot)$, define $w_{ij}(t) = \sum_{l=1}^s \tilde{\theta}_{ijl} \phi_l(t)$, where $\tilde{\theta}_{ijl} \sim N(0, 16l^{-7/3})$ that are i.i.d across i and j . The processes are given based on the autoregressive relationship,

$$x_{ij}(t) = \sum_{j'=1}^p \varrho^{|j-j'|} j^{-1/q} w_{ij'}(t) = \sum_{l=1}^s \sum_{j'=1}^p \varrho^{|j-j'|} j^{-1/q} \tilde{\theta}_{ij'l} \phi_l(t) = \sum_{l=1}^s \theta_{ijl} \phi_l(t),$$

with $\theta_{ijl} = \sum_{j'=1}^p \varrho^{|j-j'|} j^{-1/q} \tilde{\theta}_{ij'l}$. The constant q determines the sparsity level and ϱ controls the correlation among functional variables. Set $q = 0.5$ and $\varrho = 0.5$. Let $p = 50, 100, 200$, respectively, for different experiments.

To demonstrate the performance, we use the mean square error (MSE) for eigenfunctions $\|\boldsymbol{\psi} - \hat{\boldsymbol{\psi}}\|_{\mathbb{H}}^2 = \sum_{j=1}^p \|\psi_j - \hat{\psi}_j\|^2$ and the mean relative square error (MRSE) for true curves \boldsymbol{x}_i ,

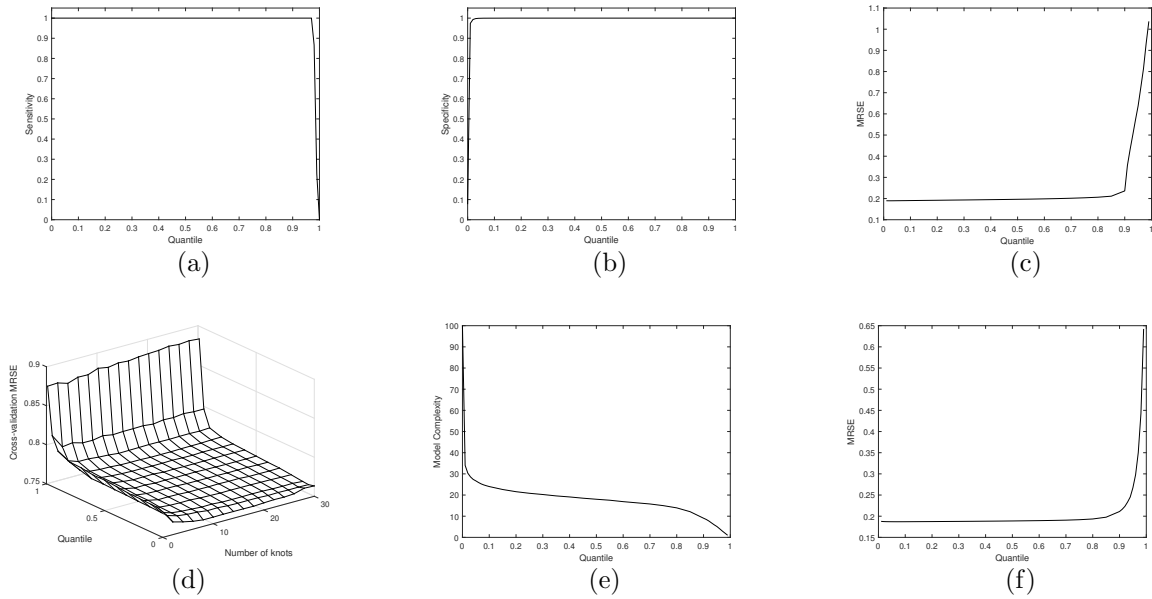


Figure 1: The results for the l_0 sparsity setting on sensitivity (a), specificity (b) and MRSE (c), where $p=100$, $g=10$. The results for the weak l_q sparsity setting with $p = 100$: cross-validated MRSE under different quantile levels and different numbers of knots (d), model complexity (i.e., the number of retained processes) (e) and MRSE (f) under different quantile levels.

$n^{-1} \sum_{i=1}^n \|\mathbf{x}_i(t) - \hat{\mathbf{x}}_i(t)\|_{\square}^2 / \|\mathbf{x}_i\|_{\square}^2$. To evaluate the correct selection performance under the l_0 sparsity, we use the specificity and sensitivity criteria, defined as Specificity = $TN/(TN + FP)$, Sensitivity = $TP/(TP + FN)$, where TP and TN are abbreviations for true positives and true negatives, respectively, i.e., the number of processes containing signals and the rest processes correctly identified by our method, similarly FP and FN stand for false positives and false negatives. Under the weak l_q sparsity, we use the number of retained processes to evaluate the model complexity. Moreover, we compare the results and computation time of our method to those of the HG method (Happ and Greven, 2018).

We use orthonormal cubic spline basis for both methods. Only results with $p = 100$ are reported, while other results revealing similar patterns are not presented for conciseness. As for the parameters s_n and ρ in our method, it is computationally expensive to use cross-

Table 1: The MSE with standard errors in parentheses for the first 4 eigenfunctions and the comparison of average computation time for a full sample recovery, where the quantile $\rho = 0.5$ in our method.

		ψ_1	ψ_2	ψ_3	ψ_4
$l_0: p = 100, g = 10$	sFPCA	.057(.005)	.087(.019)	.127(.038)	.239(.134)
	MFPCA	.072(.006)	.155(.023)	.286(.043)	.493(.116)
Weak $l_q: p = 100$	sFPCA	.007(.005)	.031(.024)	.074(.046)	.242(.255)
	MFPCA	.013(.005)	.059(.024)	.148(.047)	.381(.271)
Average computation times for recovery (second)					
	s_n	14	24	34	44
$l_0: p = 100, g = 10$	sFPCA	1.220	2.018	3.052	4.440
	MFPCA	10.55	28.04	70.04	141.1
Weak $l_q: p = 100$	sFPCA	1.269	2.099	3.210	4.464
	MFPCA	7.366	26.52	68.68	139.4

validation to choose both jointly. Based on our experience, the results are actually not sensitive to s_n , as long as it is adequate, shown in Figure 1(d), but not too large for effective computation. This empirical finding is in line with our theory that it suffices to have an adequately large s_n . In particular, we use $s_n = 54$ in the l_0 setting and $s_n = 14$ in the the l_q setting for presented results.

In such unsupervised problems, the influence of quantiles on the trade-off between the model complexity and quality of estimation/recovery is of main interest. In the l_0 sparsity setting, when the underlying complexity is known, the Specificity and Sensitivity analyses in Figures 1(a) and 1(b) clearly support an adequate choice of ρ that covers a broad range to yield correct selection. Moreover, the performance of recovery is quite stable with suitable ρ as shown in Figure 1(c). In the l_q sparsity setting, we obtain parsimonious models with

satisfactory performance of recovery over a wide quantile range, see Figures 1(e) and 1(f). As a practical advice, we suggest to choose a slightly large ρ if model parsimony is of main concern. Briefly, in practice, we suggest first fix an adequately large s_n and then determine the “best” choice of ρ . One might inspect performances of a few s_n given the selected quantiles for confirmation.

We see from Table 1 that our method with $\rho = 0.5$ clearly outperforms the HG method under both sparsity settings. In comparison with sFPCA, the HG method includes all processes, which cannot yield parsimonious representations. Lastly we illustrate substantial computational savings of our algorithm by reporting the average computation time over 100 Monte Carlo runs for a full sample recovery using different numbers of basis functions on a standard computer with 2.40GHz I7 Intel microprocessor and 16GB of memory, see Table 1. The results roughly agree with the computation complexity $O(nps_n + nN^2 + N^3)$ for our approach and $O(np^2s_n^2 + p_n^3s_n^3)$ for the HG method in Section 2, where $N = \sum_{j=1}^p N_j$ quantifies the number of all retained coefficients after thresholding that often entails $N \ll ps_n$.

4.2 Classification

We inspect the performance of our algorithm on subsequent classification. The data are generated from $y_{ij}^{(\ell)}(t_{ijk}) = \mu_j^{(\ell)}(t) + x_{ij}^{(\ell)}(t_{ijk}) + \epsilon_{ijk}$ where $\ell = 1$ or 0 denotes class 1 or 0, respectively. Let κ denote the number of significant processes for classification. We set $\mu_j^{(0)}(t) = 0$ for $j = 1, \dots, p$ and $\mu_j^{(1)}(t)$ are linear combinations of the first 5 eigen-functions with weights equal to $(1, 1, -0.75, 0.75, 0.5)$ for $j = 1, \dots, \kappa$, and the rest $\mu_j^{(1)}(t) = 0$ for $j = \kappa + 1, \dots, p$. We set $\kappa = 2$ and $p = 100$. The coefficients $\{\theta_{ijl}^{(\ell)}\}$ for both groups follow the previous generation mechanisms with slight modification. The l_0 sparsity: $D_{\nu\nu} = 3\nu^{-2}, \nu = 1, \dots, gs, g = 2$. The weak l_q sparsity: $\tilde{\theta}_{jl}^{(\ell)} \sim N(0, 3l^{-2}), j = 1, \dots, p, l = 1, \dots, s$. In each of 100 Monte Carlo runs, we generate a training set of 100 subjects and an independent testing set of 200 subjects, where half of these belong to each class. The proposed method and HG method both obtain r_n multivariate scores $\hat{\eta}_{ik} = \sum_{j=1}^p \int_0^1 y'_{ij}(t) \hat{\psi}_{kj}(t) dt$ which are low-dimensional and allow to apply the classical linear discriminant analysis (LDA) for classification. We

Table 2: The averages of misclassification rates on testing samples with standard errors in parentheses across different r_n and the average computation time. Also in square brackets shown are the average model complexity of the proposed method with standard errors in parentheses.

	Method	r_n					Time (second)
		2	5	8	12	15	
l_0	sFPCA	22.80(4.07)	9.95(2.51)	9.84(2.42)	9.97(2.49)	9.94(2.48)	1.92
	+LDA	[2.00(.00)]	[2.01(.10)]	[2.00(.00)]	[2.00(.00)]	[2.00(.00)]	
	MFPCA	27.16(4.50)	18.57(4.14)	18.15(4.13)	17.96(4.18)	17.58(4.02)	51.90
	+LDA						
	UFPCA	29.11(6.02)	11.98(6.34)	11.43(5.56)	11.53(5.48)	11.55(5.46)	43.15
	+ROAD						
Weak l_q	sFPCA	30.19(3.78)	13.41(2.79)	13.14(2.68)	13.66(2.78)	14.09(2.82)	1.28
	+LDA	[2.62(4.88)]	[2.47(5.59)]	[2.49(5.41)]	[2.54(6.26)]	[2.62(6.48)]	
	MFPCA	30.66(3.83)	15.55(2.77)	14.75(2.74)	14.67(2.79)	14.68(2.59)	7.78
	+LDA						
	UFPCA	34.27(5.77)	17.53(8.31)	16.46(8.04)	16.53(7.83)	16.55(7.94)	42.05
	+ROAD						

also consider another viable method which combines and trains the scores obtained from univariate FPCA for p processes with the high-dimensional classifier ROAD proposed by Fan et al. (2012).

In the supervised problem, we tune s_n and ρ jointly by 5-fold cross-validation, and choose the parameters of other methods in a similar manner. For comprehensive comparison, we train the models by retaining 2, 5, 8, 12, 15 principal components, respectively. The principal components mean multivariate scores η_k for the first two methods and univariate scores ξ_{jk} for the last one. As shown in Table 2, the parsimonious models obtained by our method enjoy favorable classification performance. Our algorithm successfully selects relevant processes in nearly all runs, while the HG method treats all processes equally and fails to distinguish

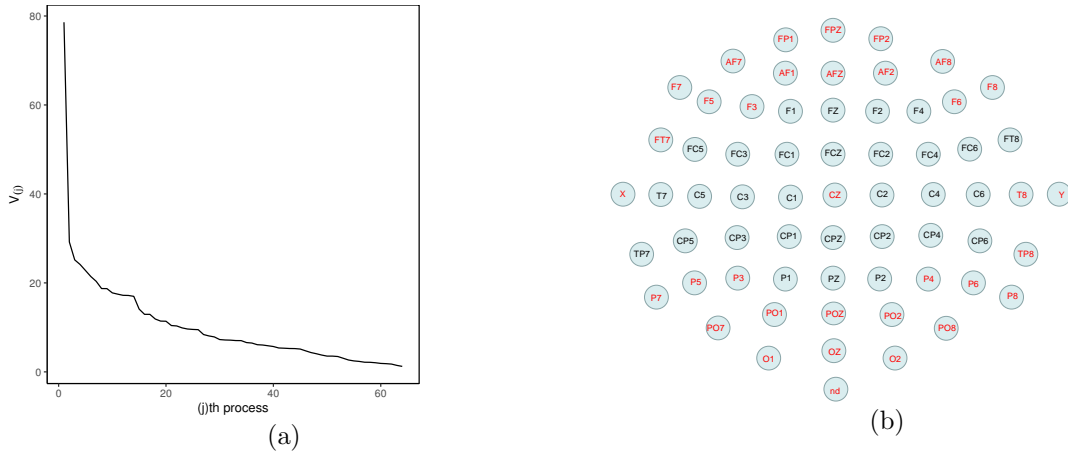


Figure 2: (a) the ordered energies $V_{(j)}$ of EEG data. (b) the electrode names and positions where the ones marked in red are selected by our method with chosen parameters over a half runs.

important processes. Although the last method adopts a high-dimensional classifier, it still performs worse than our approach. Furthermore, the average computation time over different r_n and 100 Monte Carlo runs is reported, where chosen parameters are used for our approach and the HG method, and the R package ‘fdapace’ is used for implementing the univariate FPCA. The result indicates that our proposal is much more computationally efficient for high-dimensional functional data.

5. REAL DATA EXAMPLE

We apply the proposed method to the electroencephalography (EEG) data obtained from an alcoholism study (Zhang et al., 1995; Ingber, 1997). The data consists of $n = 122$ subjects, 77 in the alcoholic group and 45 in the control group with each exposed to either a single stimulus or two stimuli. There are 64 electrodes placed at standard locations on the participants’ scalp to record the brain activities. Each electrode is sampled at 256 HZ for one second interval. Hence each subject involves $p = 64$ different functions observed at 256 time points. This dataset contains high-dimensional functional processes and was analyzed for functional graphical models (Qiao et al., 2019). Hayden et al. (2006) found evidence of

Table 3: The average misclassification rates on testing samples and computation time with standard errors in parentheses across different number of eigenfunctions. Also in square brackets shown are the average model complexity of sFPCA with standard errors in parentheses.

Method	r_n					Time (second)
	10	20	30	40	50	
sFPCA	14.25(3.98)	14.73(3.46)	13.68(3.54)	13.18(3.87)	13.28(3.55)	0.31
+LDA	[34.08(17.34)]	[36.07(19.47)]	[37.12(16.77)]	[35.19(16.64)]	[33.30(16.10)]	
MFPCA	19.38(4.53)	19.05(4.33)	18.40(4.21)	17.05(4.54)	17.33(4.34)	3.74
+LDA						
UFPCA	16.50(4.10)	16.05(4.19)	16.10(4.21)	16.10(4.21)	16.10(4.21)	364.18
+ROAD						

regional asymmetric patterns between the two groups by using 4 representative electrodes from the frontal and parietal regions.

We consider the average recordings for each subject under the single stimulus condition. As shown in Figure 2(a), the energies $V_{(j)}$ exhibit a sparsity pattern, which indicates that the sparsity assumption is advisable in practice for high-dimensional functional data. Our goal is to classify alcoholic and control groups based on their recordings. For each group, we randomly select two thirds of participants as the training sample and the rest as the test sample. We repeat 100 times and use the three methods in simulation to evaluate the classification performance. Due to sample splitting, the sample size of training samples is rather small, especially for the control group. Thus we calculate the misclassification errors over a candidate set of parameters in each method and use the lowest for comparison. Table 3 presents the misclassification rates for all considered methods under several r_n , indicating the superiority of our method with minimal misclassification errors. Moreover, the average computation time in Table 3 demonstrates the scalability of our approach for large p and m , which is consistent with the computation complexity discussed in Remark 5. The Figure 2(b) presents the 64 electrode names and positions, and the electrodes marked in red indicate

the ones selected more than half of 100 runs by our method with chosen parameters. It is observed that the retained electrodes mainly lie in the frontal and parietal regions.

ACKNOWLEDGEMENT

Fang Yao's research is partially supported by the National Natural Science Foundation of China Grant 11871080, a Discipline Construction Fund at Peking University and Key Laboratory of Mathematical Economics and Quantitative Finance (Peking University), Ministry of Education.

SUPPLEMENTARY MATERIAL

Supplementary material available at *Statistica Sinica* online includes additional regularity conditions, auxiliary results and proofs.

REFERENCES

- Berrendero, J. R., Justel, A., and Svarc, M. (2011), "Principal components for multivariate functional data," *Computational Statistics & Data Analysis*, 55, 2619–2634.
- Bruckstein, A. M., Donoho, D. L., and Elad, M. (2009), "From sparse solutions of systems of equations to sparse modeling of signals and images," *SIAM review*, 51, 34–81.
- Cai, T. T. and Yuan, M. (2010), "Nonparametric covariance function estimation for functional and longitudinal data," *University of Pennsylvania and Georgia inistitute of technology*.
- (2011), "Optimal estimation of the mean function based on discretely sampled functional data: Phase transition," *Annals of Statistics*, 39, 2330–2355.
- Chiou, J.-M., Chen, Y.-T., and Yang, Y.-F. (2014), "Multivariate functional principal component analysis: A normalization approach," *Statistica Sinica*, 24, 1571–1596.

- Dai, X., Müller, H.-G., and Yao, F. (2017), “Optimal Bayes classifiers for functional data and density ratios,” *Biometrika*, 104, 545–560.
- Donoho, D. L. and Johnstone, I. M. (1994), “Ideal spatial adaptation by wavelet shrinkage,” *Biometrika*, 81, 425–455.
- Fan, J., Feng, Y., and Tong, X. (2012), “A road to classification in high dimensional space: the regularized optimal affine discriminant,” *Journal of the Royal Statistical Society, Series B (Statistical Methodology)*, 74, 745–771.
- Hall, P. and Horowitz, J. L. (2007), “Methodology and convergence rates for functional linear regression,” *Annals of Statistics*, 35, 70–91.
- Hall, P. and Hosseini-Nasab, M. (2006), “On properties of functional principal components analysis,” *Journal of the Royal Statistical Society, Series B (Statistical Methodology)*, 68, 109–126.
- Happ, C. and Greven, S. (2018), “Multivariate functional principal component analysis for data observed on different (dimensional) domains,” *Journal of the American Statistical Association*, 113, 649–659.
- Hayden, E. P., Wiegand, R. E., Meyer, E. T., Bauer, L. O., O’Connor, S. J., Nurnberger Jr, J. I., Chorlian, D. B., Porjesz, B., and Begleiter, H. (2006), “Patterns of regional brain activity in alcohol-dependent subjects,” *Alcoholism: Clinical and Experimental Research*, 30, 1986–1991.
- Ingber, L. (1997), “Statistical mechanics of neocortical interactions: Canonical momenta indicators of electroencephalography,” *Physical Review E*, 55, 4578.
- Jacques, J. and Preda, C. (2014), “Model-based clustering for multivariate functional data,” *Computational Statistics & Data Analysis*, 71, 92–106.

- James, G. M., Hastie, T. J., and Sugar, C. A. (2001), “Principal component models for sparse functional data,” *Biometrika*, 87, 587–602.
- Johnstone, I. M. (2001), “On the distribution of the largest eigenvalue in principal components analysis,” *Annals of statistics*, 29, 295–327.
- Johnstone, I. M. and Lu, A. Y. (2009), “On consistency and sparsity for principal components analysis in high dimensions,” *Journal of the American Statistical Association*, 104, 682–693.
- Kong, D., Xue, K., Yao, F., and Zhang, H. H. (2016), “Partially functional linear regression in high dimensions,” *Biometrika*, 103, 147–159.
- Koudstaal, M. and Yao, F. (2018), “From multiple Gaussian sequences to functional data and beyond: a Stein estimation approach,” *Journal of the Royal Statistical Society, Series B (Statistical Methodology)*, 80, 319–342.
- Müller, H.-G., Stadtmüller, U., et al. (2005), “Generalized functional linear models,” *the Annals of Statistics*, 33, 774–805.
- Müller, H.-G. and Yao, F. (2008), “Functional additive models,” *Journal of the American Statistical Association*, 103, 1534–1544.
- Qiao, X., Guo, S., and James, G. M. (2019), “Functional graphical models,” *Journal of the American Statistical Association*, 114, 211–222.
- Ramsay, J. O. and Silverman, B. W. (2005), *Functional data analysis*, Springer, New York, 2nd edition.
- Rice, J. A. and Silverman, B. W. (1991), “Estimating the mean and covariance structure nonparametrically when the data are curves,” *Journal of the Royal Statistical Society, Series B (Methodological)*, 53, 233–243.

- Rice, J. A. and Wu, C. O. (2000), “Nonparametric mixed effects models for unequally sampled noisy curves,” *Biometrics*, 57, 253–259.
- Ritter, K., Wasilkowski, G. W., Wozniakowski, H., et al. (1995), “Multivariate integration and approximation for random fields satisfying Sacks-Ylvisaker conditions,” *The Annals of Applied Probability*, 5, 518–540.
- Shen, H. and Huang, J. Z. (2008), “Sparse principal component analysis via regularized low rank matrix approximation,” *Journal of Multivariate Analysis*, 99, 1015–1034.
- Vu, V. Q. and Lei, J. (2013), “Minimax sparse principal subspace estimation in high dimensions,” *Annals of Statistics*, 41, 2905–2947.
- Wong, R. K., Li, Y., and Zhu, Z. (2019), “Partially linear functional additive models for multivariate functional data,” *Journal of the American Statistical Association*, 114, 406–418.
- Yao, F., Müller, H.-G., and Wang, J.-L. (2005a), “Functional data analysis for sparse longitudinal data,” *Journal of the American Statistical Association*, 100, 577–590.
- (2005b), “Functional linear regression analysis for longitudinal data,” *Annals of Statistics*, 33, 2873–2903.
- Zhang, X. and Wang, J.-L. (2016), “From sparse to dense functional data and beyond,” *Annals of Statistics*, 44, 2281–2321.
- Zhang, X. L., Begleiter, H., Porjesz, B., Wang, W., and Litke, A. (1995), “Event related potentials during object recognition tasks,” *Brain Research Bulletin*, 38, 531–538.
- Zou, H., Hastie, T., and Tibshirani, R. (2006), “Sparse principal component analysis,” *Journal of Computational and Graphical Statistics*, 15, 265–286.

Supplementary Material: SPARSE FUNCTIONAL PRINCIPAL COMPONENT ANALYSIS IN HIGH DIMENSIONS

S1. REGULARITY CONDITIONS

We state conditions necessary for theoretical analysis, in which conditions S1-S3 concern properties of underlying processes and how the functional data are sampled/observed. Conditions S1-S2 imply that X_j is a Gaussian process with continuous sample paths, which is standard in FDA literature (Hall and Horowitz, 2007; Kong et al., 2016). Condition S3 can be directly generalized to more general designs by defining $\delta = \sup_{i,j,k} \{t_{ij,k+1} - t_{ij,k}\}$ and $m = \inf_{i,j} m_{ij}$ and assuming $\delta = O(1/m)$.

Condition S1. The basis coefficients θ_{ijl} and measurement errors ϵ_{ijk} are jointly Gaussian.

Condition S2. The sample paths are Lipschitz continuous, i.e., $|X_j(t) - X_j(s)| \leq L_{X_j}|t - s|$, and assume $E(L_{X_j}^2) < \infty$ for $j = 1, \dots, p$. Moreover, $E(\theta_{jl}^4) \leq C\{E(\theta_{jl}^2)\}^2$.

Condition S3. Let $t_k = k/m$, and the $\{t_k, k = 1, \dots, m\}$ are considered deterministic and ordered increasingly.

It is standard to assume that s_n should not be too small to capture the significant coordinates. Moreover, it should not be too large for reliable concentration results of sample variances of basis coefficients which provides theoretical foundation for establishing the thresholding rule. Thus, it suffices to have a adequately large s_n which is a useful guidance in practice. Moreover, we impose Lipschitz continuity on the basis functions without loss of generality.

Condition S4. The truncation number $\left(m^{-1}\sqrt{\log p/n}\right)^{-1/(2\alpha+1)} \ll s_n = O(p)$.

Condition S5. The basis functions are Lipschitz continuous, i.e., $|b_l(t) - b_l(s)| \leq L|t - s|$ for all $l = 1, \dots, s_n$.

We control the number of principal components r_n such that it is not too large for increasingly unstable estimates. Conditions S6 and S7 concern the approximation error and estimation error, respectively, under the weak l_q sparsity, while Conditions S8 and S9 consider the l_0 sparsity. Note that under the l_0 setting, we do not require g to be finite generally. Thus, there exists a little difference about those conditions under these two settings.

$$\text{Condition S6. } r_n^{a+1} \max \left\{ g_n^{1/2-1/q+\delta}, \left(m^{-1} \sqrt{\log p/n} \right)^{\alpha/(2\alpha+1)} \right\} = o(1) \text{ for } \delta > 0.$$

$$\text{Condition S7. } \max \left\{ r_n^{a+1} n^{-1/2}, r_n^{a+1} g_n^{1/2} m^{-1} \right\} = o(1).$$

$$\text{Condition S8. } r_n^{a+1} g \left(m^{-1} \sqrt{\log p/n} \right)^{\alpha/(2\alpha+1)} = o(1).$$

$$\text{Condition S9. } \max \left\{ r_n^{a+1} g m^{-1}, r_n^{a+1} g n^{-1/2} \right\} = o(1).$$

To ensure that the g significant processes are consistently estimable, under the l_0 case, the signals should not be too small.

$$\text{Condition S10. } \min_{j \in \{1, \dots, g\}} \max_l \sigma_{jl}^2 \gg m^{-1} \sqrt{\log p/n}.$$

S2. MORE THEORETICAL RESULTS

S2.1 Theoretical results under the l_0 sparsity

In this section, we provide theoretical results for estimating multivariate eigenfunctions under the l_0 sparsity.

Lemma S1. *Under the l_0 sparsity and Conditions 2-3, S1-S4, S10, there exists a constant $C > 0$ such that $N_j \leq C \left(m^{-1} \sqrt{\log p/n} \right)^{-1/(2\alpha+1)}$ almost surely for $j = 1, \dots, g$ and $N_j \xrightarrow{a.s.} 0$ for $j = g + 1, \dots, p$.*

Lemma S1 implies the consistent selection property, that is, all the g processes, and only those, are selected almost surely as $n \rightarrow \infty$. Without additional assumptions on the energy, it is clear that $N_j, j = 1, \dots, g$ share the same order. From the proof of Theorems S1 and S2, we also know that

$$\|\hat{G}(s, t) - G(s, t)\|_{\mathbb{H}} = O_p \left\{ g \left(m^{-1} \sqrt{\log p/n} \right)^{\alpha/(2\alpha+1)} + g n^{-1/2} + g m^{-1} \right\}.$$

These three parts in the rates of convergence correspond to bias caused by thresholding, covariance estimation error and discretization error, respectively. Consequently, the rates of convergence for estimated eigenfunctions are obtained, and presented as approximation and estimation error, respectively.

Theorem S1 (Approximation Error). *Under the l_0 sparsity, if Conditions 1-3, S1-S4, S8 and S10 hold and $\langle \boldsymbol{\psi}_k, \tilde{\boldsymbol{\psi}}_k \rangle_{\mathbb{H}} \geq 0$, then uniformly for $k = 1, \dots, r_n$,*

$$\|\tilde{\boldsymbol{\psi}}_k - \boldsymbol{\psi}_k\|_{\mathbb{H}} = O \left\{ k^{a+1} g \left(m^{-1} \sqrt{\log p/n} \right)^{\alpha/(2\alpha+1)} \right\}, \quad a.s..$$

The approximation error is caused by excluding the small variances in the subset selection step. Due to the correct selection property, this error is associated with g , the number of retained coefficients N_j and the variance decaying rate α . To be specific, the term $\left(m^{-1} \sqrt{\log p/n} \right)^{\alpha/(2\alpha+1)}$, i.e., $N_j^{-\alpha}$, is determined by excluding coordinates with small variances and the additional term k^{a+1} is attributed to the increasing error of approximating higher order eigenelements $\boldsymbol{\psi}_k, k = 1, \dots, r_n$. Next we quantify the estimation error, where we consider two cases depending on whether the discretization error can be asymptotically negligible. Recall that γ quantifies the sampling rate $m = O(n^\gamma)$, where $\gamma > (1 - \beta)/2$ and $p = O\{\exp(n^\beta)\}$ for $0 < \beta < 1$.

Theorem S2 (Estimation Error). *Under the l_0 sparsity, if Conditions 1-3, S1- S5, S9-S10 hold and $\langle \hat{\boldsymbol{\psi}}_k, \tilde{\boldsymbol{\psi}}_k \rangle_{\mathbb{H}} \geq 0$, then uniformly for $k = 1, \dots, r_n$, we have the following.*

Case 1. When $\gamma > 1/2$,

$$\|\tilde{\boldsymbol{\psi}}_k - \hat{\boldsymbol{\psi}}_k\|_{\mathbb{H}} = O_p \left(k g n^{-1/2} \right).$$

Case 2. When $(1 - \beta)/2 < \gamma \leq 1/2$,

$$\|\tilde{\boldsymbol{\psi}}_k - \hat{\boldsymbol{\psi}}_k\|_{\mathbb{H}} = O_p \left(k^{a+1} g m^{-1} \right).$$

The correct selection property implied by Lemma S1 makes it sufficient to consider the estimation error of a small set of retained processes. Note that the estimation error does

not involve the term N_j , as we quantify the discretization error of retained coefficients via retained processes using Bessel's inequality. The sampling rate γ plays an important role in the rates of convergence, which exhibits the phase transition phenomenon at $\gamma = 0.5$. For more detailed interpretation, one can refer to the discussion following Theorems 1-2.

S2.2 Theoretical results on recovery

We can represent the trajectories using estimated eigenfunctions. It is of interest to investigate the theoretical performance of recovered processes. To provide more insights of the sampling frequency of m on the results, we directly characterize the discretization error. For recovered curves, one has the following decomposition:

$$\|\hat{\mathbf{x}} - \mathbf{x}\|_{\mathbb{H}} \leq \|\mathbf{x}^{r_n} - \mathbf{x}\|_{\mathbb{H}} + \|\tilde{\mathbf{x}}^{r_n} - \mathbf{x}^{r_n}\|_{\mathbb{H}} + \|\hat{\mathbf{x}} - \tilde{\mathbf{x}}^{r_n}\|_{\mathbb{H}},$$

where $\hat{\mathbf{x}}^{r_n} = \sum_{k=1}^{r_n} \hat{\eta}_k \hat{\boldsymbol{\psi}}_k$, $\tilde{\mathbf{x}}^{r_n} = \sum_{k=1}^{r_n} \tilde{\eta}_k \tilde{\boldsymbol{\psi}}_k$ and $\mathbf{x}^{r_n} = \sum_{k=1}^{r_n} \eta_k \boldsymbol{\psi}_k$. In the righthand, the first and second terms can be both viewed as approximation errors, while the third term is seen as an estimation error. Denote $\tilde{\eta}_k = \langle \tilde{\mathbf{x}}, \tilde{\boldsymbol{\psi}}_k \rangle_{\mathbb{H}}$.

Theorem S3 (Approximation Error under l_0). *Under Conditions in Theorem S1, if $\langle \boldsymbol{\psi}_k, \tilde{\boldsymbol{\psi}}_k \rangle_{\mathbb{H}} \geq 0$, then uniformly for $k = 1, \dots, r_n$,*

$$|\tilde{\eta}_k - \eta_k| = O_p \left\{ k^{a+1} g^{3/2} \left(m^{-1} \sqrt{\log p/n} \right)^{\frac{\alpha}{2\alpha+1}} \right\},$$

Moreover,

$$\begin{aligned} \|\mathbf{X} - \mathbf{X}^{r_n}\|_{\mathbb{H}} &= O_p \left(g r_n^{1-a} \right), \\ \|\tilde{\mathbf{X}}^{r_n} - \mathbf{X}^{r_n}\|_{\mathbb{H}} &= O_p \left\{ r_n^{a+3/2} g^{3/2} \left(m^{-1} \sqrt{\log p/n} \right)^{\frac{\alpha}{2\alpha+1}} \right\}. \end{aligned}$$

Theorem S4 (Estimation error under l_0). *Under Conditions in Theorem S2, if $\langle \hat{\boldsymbol{\psi}}_k, \tilde{\boldsymbol{\psi}}_k \rangle_{\mathbb{H}} \geq 0$, then uniformly for $k = 1, \dots, r_n$,*

Case 1. When $\gamma > 1/2$,

$$|\tilde{\eta}_{ik} - \hat{\eta}_{ik}| = O_p \left(k g^{3/2} n^{-1/2} + k^{a/2} g m^{-1/2} \right),$$

$$\|\tilde{\mathbf{x}}_i^{r_n} - \hat{\mathbf{x}}_i^{r_n}\|_{\mathbb{H}} = O_p \left(r_n^{3/2} g^{3/2} n^{-1/2} + r_n^{(a+1)/2} g m^{-1/2} \right), \quad i = 1, \dots, n.$$

Case 2. When $(1 - \beta)/2 < \gamma \leq 1/2$,

$$|\tilde{\eta}_{ik} - \hat{\eta}_{ik}| = O_p \left(k^{a+1} g^{3/2} m^{-1} + k^{a/2} g m^{-1/2} \right),$$

$$\|\tilde{\mathbf{x}}_i^{r_n} - \hat{\mathbf{x}}_i^{r_n}\|_{\mathbb{H}} = O_p \left(r_n^{a+3/2} g^{3/2} m^{-1} + r_n^{(a+1)/2} g m^{-1/2} \right), \quad i = 1, \dots, n.$$

It is much more straightforward to quantify the approximation error based on Theorem S1. For estimation error, we need to carefully investigate both the discretization and measurement errors. Basically, the first term in the rates of convergence mainly depend on the estimation of eigenfunctions, and the additional term is attributed to the measurement error. For consistent estimators of scores and recovery, we assume $\alpha > 1/2$. Moreover, under the weak l_q sparsity, we consider the most interesting case where $0 < q < 1$ (Bruckstein et al., 2009). For more detailed interpretation, one can refer to the discussion following Theorems 1-2.

Theorem S5 (Approximation Error under weak l_q). *Under the Conditions in Theorem 1, if $\langle \boldsymbol{\psi}_k, \tilde{\boldsymbol{\psi}}_k \rangle_{\mathbb{H}} \geq 0$, then uniformly for $k = 1, \dots, r_n$,*

Case 1. When $q(\alpha + 1) > 2$,

$$\begin{aligned} |\tilde{\eta}_k - \eta_k| &= O_p \left(k^{a+1} g_n^{1/2-1/q} \right), \\ \|\tilde{\mathbf{X}}^{r_n} - \mathbf{X}^{r_n}\|_{\mathbb{H}} &= O_p \left(r_n^{a+3/2} g_n^{1/2-1/q} \right). \end{aligned}$$

Case 2. When $q(\alpha + 1) = 2$,

$$\begin{aligned} |\tilde{\eta}_k - \eta_k| &= O_p \left\{ k^{a+1} (m^{-1} \sqrt{\log p/n})^{\alpha/(2\alpha+1)} (\log g_n)^{1/2} \right\}, \\ \|\tilde{\mathbf{X}}^{r_n} - \mathbf{X}^{r_n}\|_{\mathbb{H}} &= O_p \left\{ r_n^{a+3/2} (m^{-1} \sqrt{\log p/n})^{\alpha/(2\alpha+1)} (\log g_n)^{1/2} \right\}. \end{aligned}$$

Case 3. When $q(\alpha + 1) < 2$,

$$\begin{aligned} |\tilde{\eta}_k - \eta_k| &= O_p \left\{ k^{a+1} (m^{-1} \sqrt{\log p/n})^{\alpha/(2\alpha+1)} \right\}, \\ \|\tilde{\mathbf{X}}^{r_n} - \mathbf{X}^{r_n}\|_{\mathbb{H}} &= O_p \left\{ r_n^{a+3/2} (m^{-1} \sqrt{\log p/n})^{\alpha/(2\alpha+1)} \right\}, \end{aligned}$$

Moreover,

$$\|\mathbf{X} - \mathbf{X}^{r_n}\|_{\mathbb{H}} = O_p(r_n^{1-a}).$$

Theorem S6 (Estimation Error under weak l_q). *Under Conditions in Theorem 2, if $\langle \hat{\boldsymbol{\psi}}_k, \tilde{\boldsymbol{\psi}}_k \rangle_{\mathbb{H}} > 0$, then uniformly for $k = 1, \dots, r_n$,*

Case 1. When $\gamma > 1/(2 - q)$,

$$|\tilde{\eta}_{ik} - \hat{\eta}_{ik}| = O_p(kn^{-1/2} + k^{a/2}m^{-1/2}),$$

$$\|\tilde{\boldsymbol{x}}_i^{r_n} - \hat{\boldsymbol{x}}_i^{r_n}\|_{\mathbb{H}} = O_p(r_n^{3/2}n^{-1/2} + r_n^{(a+1)/2}m^{-1/2}), \quad i = 1, \dots, n.$$

Case 2. When $(1 - \beta)/2 < \gamma \leq 1/(2 - q)$,

$$|\tilde{\eta}_{ik} - \hat{\eta}_{ik}| = O_p(k^{a+1}g_n^{1/2}m^{-1} + k^{a/2}m^{-1/2}),$$

$$\|\tilde{\boldsymbol{x}}_i^{r_n} - \hat{\boldsymbol{x}}_i^{r_n}\|_{\mathbb{H}} = O_p(r_n^{a+3/2}g_n^{1/2}m^{-1} + r_n^{(a+1)/2}m^{-1/2}), \quad i = 1, \dots, n.$$

S3. PROOFS OF MAIN RESULTS

Proof of Proposition 1. We provide the proof of the generalized version of Proposition 1 which allows different basis functions among processes. The univariate orthonormal basis representation for each random process is $X_j = \sum_{l=1}^{\infty} \theta_{jl} b_{jl}$. Recall that $G(s, t) = E\{\mathbf{X}(s)\mathbf{X}(t)^{\top}\} \in \mathbb{R}^{p \times p}$ and $\int G(s, t)\boldsymbol{\psi}_k(s)ds = \lambda_k \boldsymbol{\psi}_k(t)$. Then we have

$$\begin{aligned} \left\{ \int G(s, t)\boldsymbol{\psi}_k(s)ds \right\}_j &= \sum_{j'=1}^p \int \text{cov}\{X_{j'}(s), X_j(t)\} \boldsymbol{\psi}_{kj'}(s) ds \\ &= \sum_{j'=1}^p \int \sum_{l'=1}^{\infty} \sum_{m=1}^{\infty} \text{cov}(\theta_{j'l'}, \theta_{jm}) b_{j'l'}(s) b_{jm}(t) \boldsymbol{\psi}_{kj'}(s) ds \\ &= \sum_{j'=1}^p \sum_{l'=1}^{\infty} \sum_{m=1}^{\infty} \text{cov}(\theta_{j'l'}, \theta_{jm}) b_{jm}(t) \int b_{j'l'}(s) \boldsymbol{\psi}_{kj'}(s) ds \\ &= \lambda_k \boldsymbol{\psi}_{kj}(t). \end{aligned} \tag{S1}$$

Denote $u_{kjl} = \int_{\mathcal{T}} b_{jl}(t)\boldsymbol{\psi}_{kj}(t)dt$. Multiplying both sides by $b_{jl}(t)$ and then integrating both sides over t yields

$$\sum_{j'=1}^p \sum_{l'=1}^{\infty} \sum_{m=1}^{\infty} \text{cov}(\theta_{j'l'}, \theta_{jm}) \int b_{jm}(t)b_{jl}(t)dt \int b_{j'l'}(s)\boldsymbol{\psi}_{kj'}(s)ds = \lambda_k \int b_{jl}(t)\boldsymbol{\psi}_{kj}(t)dt,$$

$$\sum_{j'=1}^p \sum_{l'=1}^{\infty} \text{cov}(\theta_{j'l'}, \theta_{jl}) u_{kj'l'} = \lambda_k u_{kjl}. \quad (\text{S2})$$

Combining (S1) and (S2), the eigenfunctions $\boldsymbol{\psi}_k$ are

$$\psi_{kj}(t) = \sum_{l=1}^{\infty} u_{kjl} b_{jl}(t), \quad t \in \mathcal{T}, j = 1, \dots, p, k = 1, 2, \dots$$

Obviously, $\sum_{j=1}^p \sum_{l=1}^{\infty} u_{kjl}^2 = 1$ and $\sum_{j=1}^p \sum_{l=1}^{\infty} u_{kjl} u_{k'jl} = 0$ for $k \neq k'$. And the scores are

$$\begin{aligned} \eta_k &= \langle \mathbf{X}(t), \boldsymbol{\psi}_k(t) \rangle = \sum_{j=1}^p \int X_j(t) \psi_{kj}(t) dt \\ &= \sum_{j=1}^p \int \sum_{l=1}^{\infty} \theta_{jl} b_{jl}(t) \psi_{kj}(t) dt = \sum_{j=1}^p \sum_{l=1}^{\infty} \theta_{jl} u_{kjl}. \end{aligned}$$

□

For convenience, we suppress the subscript \mathbb{H} in inner product and norm operations when there is no ambiguity.

Proof of Theorem 1. Recall that $\tilde{X}_j = \sum_{l=1}^{N_j} \theta_{jl} b_l$ and $\tilde{G}(s, t) = E\{\tilde{\mathbf{X}}(s)\tilde{\mathbf{X}}(t)^{\text{T}}\}$, $\tilde{\lambda}_k$ and $\tilde{\boldsymbol{\psi}}_k$ are corresponding eigenvalues and eigenfunctions respectively. First we provide the bound of $\|\tilde{G} - G\|^2$ which is important in the sequel.

$$\begin{aligned} \|\tilde{G} - G\|^2 &\leq \int \int \sum_{j=1}^p \sum_{j'=1}^p \{ \tilde{G}_{jj'}(s, t) - G_{jj'}(s, t) \}^2 ds dt \\ &= \int \int \sum_{j=1}^p \sum_{j'=1}^p \{ E\tilde{X}_j(s)\tilde{X}_{j'}(t) - EX_j(s)X_{j'}(t) \}^2 ds dt \\ &\lesssim \sum_{j=1}^p \sum_{j'=1}^p \left(\int \int [E\tilde{X}_j(s)\{\tilde{X}_{j'}(t) - X_{j'}(t)\}]^2 ds dt \right. \\ &\quad \left. + \int \int [EX_{j'}(t)\{\tilde{X}_j(s) - X_j(s)\}]^2 ds dt \right) \\ &\leq E\|\tilde{\mathbf{X}}\|^2 E\|\tilde{\mathbf{X}} - \mathbf{X}\|^2 + E\|\mathbf{X}\|^2 E\|\tilde{\mathbf{X}} - \mathbf{X}\|^2. \end{aligned} \quad (\text{S3})$$

Use the notations I_n^- and I_n^+ defined in Lemma S2. Denote the event $\{I_n^- \subset \hat{I} \subset I_n^+\}$ by A_n . By Lemma S2, we have $P(\limsup A_n) = 1$. Under the weak l_q sparsity, $E\|\mathbf{X}\|^2 = O(1)$. On the event A_n , we have

$$E\|\tilde{\mathbf{X}} - \mathbf{X}\|^2 \leq \sum_{(j,l) \notin I_n^-} \sigma_{jl}^2 \asymp \sum_{j=1}^{g_n} \sum_{l=N_j+1}^{\infty} \sigma_{jl}^2 + \sum_{j=g_n+1}^p V_j = I + II.$$

It is obtained that $II = O(g_n^{1-2/q})$. Based on the weak l_q sparsity and Lemma 1, we have

$$I \asymp \sum_{j=1}^{g_n} j^{-\frac{2}{q(2\alpha+1)}} \left(\frac{1}{m} \sqrt{\frac{\log p}{n}} \right)^{2\alpha/(2\alpha+1)}.$$

Next we consider the following cases about the first term I based on relationship between two types of sparsity q and α to obtain the final results.

- If $q(2\alpha + 1) > 2$, then $I = O \left[\{m^{-1}(\log p/n)^{1/2}\}^{2\alpha/(2\alpha+1)} g_n^{1-2/q(2\alpha+1)} \right] = O(g_n^{1-2/q})$.

Combining I and II yields $E\|\tilde{\mathbf{X}} - \mathbf{X}\|^2 = O(g_n^{1-2/q})$.

- If $q(2\alpha + 1) = 2$, then

$$I = \{m^{-1}(\log p/n)^{1/2}\}^{2\alpha/(2\alpha+1)} \sum_{j=1}^{g_n} j^{-1} = O \left[\{m^{-1}(\log p/n)^{1/2}\}^{2\alpha/(2\alpha+1)} \log(g_n) \right].$$

Combining I and II yields $E\|\tilde{\mathbf{X}} - \mathbf{X}\|^2 = O \left[\{m^{-1}(\log p/n)^{1/2}\}^{2\alpha/(2\alpha+1)} \log(g_n) \right]$.

- If $q(2\alpha + 1) < 2$, then we have $I = O \left[\{m^{-1}(\log p/n)^{1/2}\}^{2\alpha/(2\alpha+1)} \right]$. Combining I and

II yields $E\|\tilde{\mathbf{X}} - \mathbf{X}\|^2 = O \left[\{m^{-1}(\log p/n)^{1/2}\}^{2\alpha/(2\alpha+1)} \right]$.

From the bound on covariance (S3), according to the result of Theorem 1 in Hall and Hosseini-Nasab (2006), we arrive at the desired results. \square

Proof of Theorem 2. Recall that g_n denotes the number of retained processes. First, we prove that the measurement error is negligible and then it suffices to quantify the error $\|\tilde{G} - \hat{G}\|$ on the event A_n , where $\hat{G}_{jj'}(s, t) = n^{-1} \sum_{i=1}^n \tilde{x}_{ij}(s) \tilde{x}_{ij'}(t)$ and $\tilde{x}_{ij} = \sum_{l=1}^{N_j} \hat{\theta}_{ijl} b_l$.

Observe that

$$\tilde{\epsilon}_{ijl} = \sum_{k=1}^m \epsilon_{ijk} \int_{t_{k-1}}^{t_k} b_l(t) dt.$$

Then we have $\text{var}(\tilde{\epsilon}_{ijl}) = \sigma^2 \sum_{k=1}^m \left\{ \int_{t_{k-1}}^{t_k} b_l(t) dt \right\}^2$.

Denote $\tilde{\Delta} = \text{diag}(\text{var}(\tilde{\epsilon}_{11}), \dots, \text{var}(\tilde{\epsilon}_{1N_1}), \dots, \text{var}(\tilde{\epsilon}_{p1}), \dots, \text{var}(\tilde{\epsilon}_{pN_p}))$ and Δ is a $N \times N$ diagonal matrix whose elements are all $1/m$ where $N = \sum_{j=1}^p N_j$. Note that

$$\left| \sum_{k=1}^m \left\{ \int_{t_{k-1}}^{t_k} b_l(t) dt \right\}^2 - \frac{1}{m} \right|$$

$$\begin{aligned}
&= \left| \sum_{k=1}^m \int_{t_{k-1}}^{t_k} \int_{t_{k-1}}^{t_k} b_l(t) \{b_l(s) - b_l(t)\} dt ds \right| \\
&\leq \frac{L}{m^2} \int_0^1 b_l(t) dt,
\end{aligned}$$

where the last inequality follows from the Condition S5. Note that from Lemma 1 and under Condition 3, we have $\|\tilde{\Delta} - \Delta\|_F = o_p(g_n^{1/2} m^{-1})$.

On the event A_n ,

$$\begin{aligned}
\|\tilde{G} - \hat{G}\|^2 &= \int \int \sum_{j=1}^p \sum_{j'=1}^p \{ \tilde{G}_{jj'}(s, t) - \hat{G}_{jj'}(s, t) \}^2 ds dt \\
&= \int \int \sum_{j=1}^p \sum_{j'=1}^p \left\{ n^{-1} \sum_{i=1}^n \tilde{x}_{ij}(s) \tilde{x}_{ij'}(t) - n^{-1} \sum_{i=1}^n \tilde{x}_{ij}(s) \tilde{x}_{ij'}(t) \right. \\
&\quad \left. + n^{-1} \sum_{i=1}^n \tilde{x}_{ij}(s) \tilde{x}_{ij'}(t) - E \tilde{X}_j(s) \tilde{X}_{j'}(t) \right\}^2 ds dt \\
&\leq 4 \sum_{j=1}^{g_n} \sum_{j'=1}^{g_n} \int \int \left[n^{-1} \sum_{i=1}^n \{ \tilde{x}_{ij}(s) - \tilde{x}_{ij}(s) \} \tilde{x}_{ij'}(t) \right]^2 ds dt \\
&\quad + 4 \sum_{j=1}^{g_n} \sum_{j'=1}^{g_n} \int \int \left[n^{-1} \sum_{i=1}^n \tilde{x}_{ij}(s) \{ \tilde{x}_{ij'}(t) - \tilde{x}_{ij'}(t) \} \right]^2 ds dt \\
&\quad + 2 \int \int \sum_{j=1}^{g_n} \sum_{j'=1}^{g_n} \left\{ n^{-1} \sum_{i=1}^n \tilde{x}_{ij}(s) \tilde{x}_{ij'}(t) - E \tilde{X}_j(s) \tilde{X}_{j'}(t) \right\}^2 ds dt \\
&= I + II + III. \tag{S4}
\end{aligned}$$

To bound the term I and II, note that

$$\begin{aligned}
&\int \int \left[n^{-1} \sum_{i=1}^n \{ \tilde{x}_{ij}(s) - \tilde{x}_{ij}(s) \} \tilde{x}_{ij'}(t) \right]^2 ds dt \\
&\leq n^{-2} \left(\sum_{i=1}^n \left[\int \int \{ \tilde{x}_{ij}(s) - \tilde{x}_{ij}(s) \}^2 \tilde{x}_{ij'}^2(t) ds dt \right]^{1/2} \right)^2 \\
&= n^{-2} \left(\sum_{i=1}^n \left[\|\tilde{x}_{ij} - \tilde{x}_{ij}\|_{L^2} \left\{ \int \tilde{x}_{ij'}(t)^2 dt \right\}^{1/2} \right] \right)^2, \tag{S5}
\end{aligned}$$

where the first inequality follows from the triangle inequality. Similarly, we have

$$\int \int \left[n^{-1} \sum_{i=1}^n \tilde{x}_{ij}(s) \{ \tilde{x}_{ij'}(t) - \tilde{x}_{ij'}(t) \} \right]^2 ds dt$$

$$\leq n^{-2} \left(\sum_{i=1}^n \left[\|\tilde{x}_{ij'} - \check{x}_{ij'}\|_{L^2} \left\{ \int \tilde{x}_{ij}^2(s) ds \right\}^{1/2} \right] \right)^2. \quad (\text{S6})$$

Using Bessel's inequality and Condition S2, we may prove that

$$\|\tilde{x}_{ij} - \check{x}_{ij}\|_{L^2} \leq \|x'_{ij} - x_{ij}\|_{L^2} = O_p \left(\frac{1}{m} \right). \quad (\text{S7})$$

So we have $I = O_p(g_n/m^2)$ and $II = O_p(g_n/m^2)$. To bound the term III,

$$\begin{aligned} & n^{-2} \int \int E \left\{ \sum_{i=1}^n \{ \tilde{x}_{ij}(s) \tilde{x}_{ij'}(t) - E \tilde{X}_j(s) \tilde{X}_{j'}(t) \} \right\}^2 ds dt \\ & \leq n^{-2} \int \int \sum_{i=1}^n E \{ \tilde{x}_{ij}^2(s) \tilde{x}_{ij'}^2(t) \} ds dt \\ & = O_p \left(\frac{1}{n} \right), \end{aligned}$$

where the last equality follows from Condition S2. Thus, combining together yields that $|||\hat{G} - \tilde{G}||| = O_p(n^{-1/2} + g_n^{1/2} m^{-1})$.

Case 1. If $\gamma > 1/(2-q)$, the parametric rate dominates while the discretization error is negligible, $|||\tilde{G} - \hat{G}||| = O_p(n^{-1/2})$. In this case, we adopt techniques in Hall and Horowitz (2007) and Kong et al. (2016) to obtain sharper bounds.

Define $\hat{\Delta} = |||\hat{G} - \tilde{G}|||$. We find that, for $k = 1, \dots, r_n$,

$$\tilde{\lambda}_k - \tilde{\lambda}_{k+1} \geq |\lambda_k - \lambda_{k+1} - 2\Delta| \geq Ck^{-a-1},$$

where $\Delta = |||G - \tilde{G}|||$. Denote

$$\mathcal{J}_n = \{ \tilde{\lambda}_k - \tilde{\lambda}_{k+1} > 2/(2 - \sqrt{2})\hat{\Delta}, k = 1, \dots, r_n \}.$$

The set \mathcal{J}_n means that the distance of adjacent ordered eigenvalues does not fall below $2/(2 - \sqrt{2})\hat{\Delta}$, $P(\mathcal{J}_n) \rightarrow 1, n \rightarrow \infty$ is implied by Condition S9. For some constant C , define the set

$$\mathcal{F}_n = \{ (\hat{\lambda}_{k_1} - \tilde{\lambda}_{k_2})^{-2} \leq 2(\tilde{\lambda}_{k_1} - \tilde{\lambda}_{k_2})^{-2} \leq Cr_n^{2(a+1)}, k_1, k_2 = 1, \dots, r_n, k_1 \neq k_2 \}.$$

For $k_1 \neq k_2$, $|\hat{\lambda}_{k_1} - \tilde{\lambda}_{k_1}| \leq \hat{\Delta} < (1 - \sqrt{2}/2) \min_{k_1 \neq k_2} |\tilde{\lambda}_{k_1} - \tilde{\lambda}_{k_2}|$ gives that

$$\begin{aligned} |\hat{\lambda}_{k_1} - \tilde{\lambda}_{k_2}| &= |\hat{\lambda}_{k_1} - \tilde{\lambda}_{k_1} + \tilde{\lambda}_{k_1} - \tilde{\lambda}_{k_2}| \\ &\geq |\tilde{\lambda}_{k_1} - \tilde{\lambda}_{k_2}| - |\hat{\lambda}_{k_1} - \tilde{\lambda}_{k_1}| \\ &\geq |\tilde{\lambda}_{k_1} - \tilde{\lambda}_{k_2}| - \hat{\Delta}. \end{aligned}$$

Then we have $P(\mathcal{F}_n) \rightarrow 1$ as $n \rightarrow \infty$. By (5.16) in Hall and Horowitz (2007), one has $\|\hat{\boldsymbol{\psi}}_k - \tilde{\boldsymbol{\psi}}_k\|^2 \leq 2\hat{u}_k^2$ where $\hat{u}_k^2 = \sum_{l:l \neq k} (\hat{\lambda}_k - \tilde{\lambda}_l)^{-2} \left\{ \int \hat{\boldsymbol{\psi}}_k^\top (\hat{G} - \tilde{G}) \tilde{\boldsymbol{\psi}}_l \right\}^2$. By Lemma 1 in Kong et al. (2016), we have

$$\hat{u}_k^2 \leq 4 \sum_{l:l \neq k} (\tilde{\lambda}_k - \tilde{\lambda}_l)^{-2} \left\{ \int \tilde{\boldsymbol{\psi}}_k^\top (\tilde{G} - \hat{G}) \tilde{\boldsymbol{\psi}}_l \right\}^2 + 2Cr_n^{2(a+1)} \|\hat{\boldsymbol{\psi}}_k - \tilde{\boldsymbol{\psi}}_k\|^2 \hat{\Delta}^2.$$

Plugging this into $\|\hat{\boldsymbol{\psi}}_k - \tilde{\boldsymbol{\psi}}_k\|^2 \leq 2\hat{u}_k^2$, we find that

$$(1 - 4Cr_n^{2(a+1)} \hat{\Delta}^2) \|\hat{\boldsymbol{\psi}}_k - \tilde{\boldsymbol{\psi}}_k\|^2 \leq 8 \sum_{l:l \neq k} (\tilde{\lambda}_k - \tilde{\lambda}_l)^{-2} \left\{ \int \tilde{\boldsymbol{\psi}}_k^\top (\tilde{G} - \hat{G}) \tilde{\boldsymbol{\psi}}_l \right\}^2.$$

As $r_n^{2(a+1)} \hat{\Delta}^2 = o_p(1)$, we have

$$\|\hat{\boldsymbol{\psi}}_k - \tilde{\boldsymbol{\psi}}_k\|^2 \leq 8 \sum_{l:l \neq k} (\tilde{\lambda}_k - \tilde{\lambda}_l)^{-2} \left\{ \int \tilde{\boldsymbol{\psi}}_k^\top (\tilde{G} - \hat{G}) \tilde{\boldsymbol{\psi}}_l \right\}^2,$$

by analogy to (5.22) in Hall and Horowitz (2007), $E \left[\sum_{l:l \neq k} (\tilde{\lambda}_k - \tilde{\lambda}_l)^{-2} \left\{ \int \tilde{\boldsymbol{\psi}}_k^\top (\tilde{G} - \hat{G}) \tilde{\boldsymbol{\psi}}_l \right\}^2 \right] = O(k^2 n^{-1})$ holds uniformly in $k = 1, \dots, r_n$.

Case 2. If $\gamma \leq 1/(2 - q)$, the discretization error dominates, $\|\hat{G} - \tilde{G}\| = O_p(g_n^{1/2} m^{-1})$.

With the result of Theorem 1 in Hall and Hosseini-Nasab (2006), the final results are established. \square

S4. PROOFS OF LEMMAS AND AUXILIARY RESULTS

Define two non-random sets $I_n^- = \{(j, l), j = 1, \dots, p; l = 1, \dots, s_n : \sigma_{jl}^2 > m^{-1} \sigma^2 a_+ \alpha_n\}$ and $I_n^+ = \{(j, l), j = 1, \dots, p; l = 1, \dots, s_n : \sigma_{jl}^2 > m^{-1} \sigma^2 a_- \alpha_n\}$. Recall that $\hat{I} = \{(j, l), j = 1, \dots, p; l = 1, \dots, s_n : \hat{\sigma}_{jl}^2 \geq m^{-1} \sigma^2 (1 + \alpha_n)\}$.

Lemma S2. *For sufficiently large n , $I_n^- \subset \hat{I} \subset I_n^+$ almost surely.*

Proof. Recall that $\tilde{\sigma}_{jl}^2 = \text{var}(\hat{\theta}_{jl})$. Observe that

$$\begin{aligned}\hat{\theta}_{ijl} &= \int_{\mathcal{T}} x_{ij}(t)b_l(t)dt + \sum_{k=1}^m \int_{t_{k-1}}^{t_k} \{x_{ij}(t_k) - x_{ij}(t)\}b_l(t)dt + \tilde{\epsilon}_{ijl} \\ &= \theta_{ijl} + z_{ijl} + \tilde{\epsilon}_{ijl}.\end{aligned}$$

We have $\tilde{\theta}_{ijl} = \theta_{ijl} + z_{ijl}$ and $\tilde{\sigma}_{jl}^2 = \sigma_{jl}^2 + \text{var}(z_{ijl}) + \text{cov}(\theta_{ijl}, z_{ijl})$. Under the Lipschitz condition, we have $\text{var}(z_{ijl}) = O(m^{-2})$. So $\tilde{\sigma}_{jl}^2 = \sigma_{jl}^2 + O(m^{-2}) + O(\sigma_{jl}/m)$. First we state the results from Johnstone (2001) that

$$\begin{aligned}\text{pr}\{\chi_n^2 \leq n(1 - \epsilon)\} &\leq \exp(-n\epsilon^2/4), \quad 0 \leq \epsilon \leq 1, \\ \text{pr}\{\chi_n^2 \geq n(1 + \epsilon)\} &\leq \exp(-3n\epsilon^2/16), \quad 0 \leq \epsilon < 1/2.\end{aligned}$$

Denote $\bar{M}_n \stackrel{d}{=} \chi_n^2/n$ where $x \stackrel{d}{=} y$ means that x has the same distribution as y . $|I|$ denotes the cardinality of set I . Then,

$$\begin{aligned}P_n^- &= \text{pr}(I_n^- \notin \hat{I}) \\ &= \text{pr}[\{(j, l) \in I_n^- : \hat{\sigma}_{jl}^2 \leq m^{-1}\sigma^2(1 + \alpha_n)\}] \\ &\leq \sum_{(j,l) \in I_n^-} \text{pr}\{\hat{\sigma}_{jl}^2 \leq m^{-1}\sigma^2(1 + \alpha_n)\}, \quad \text{subadditivity} \\ &= \sum_{(j,l) \in I_n^-} \text{pr}\{\bar{M}_n \leq (1 + \alpha_n)/(1 + m\tilde{\sigma}_{jl}^2/\sigma^2)\}, \quad \hat{\sigma}_{jl}^2 \sim (m^{-1}\sigma^2 + \tilde{\sigma}_{jl}^2)\chi_n^2/n \\ &\leq |I_n^-| \text{pr}\{\bar{M}_n \leq (1 + \alpha_n)/(1 + (1 + o(1))a_+\alpha_n)\} \\ &= |I_n^-| \text{pr}(\bar{M}_n \leq 1 - \epsilon_n), \\ &\leq |I_n^-| \exp(-n\epsilon_n^2/4),\end{aligned}$$

where $\epsilon_n = \{a_+(1+o(1))-1\}\alpha_n/\{1+(1+o(1))a_+\alpha_n\}$ and the second inequality holds because $\tilde{\sigma}_{jl}^2/\sigma_{jl}^2 \rightarrow 1$ for all $(j, l) \in I_n^-$ under Condition 3. We have $n\epsilon_n^2 \approx \{(a_+ - 1)^2\alpha_0^2 \log(ps_n)\}/(1 + a_+\alpha_n)^2 \geq (a_+ - 1)^2\alpha' \log(ps_n)$ where α' is slightly smaller than α_0^2 . Let $\alpha_+'' = (a_+ - 1)^2\alpha'/4$,

then $P_n^- \leq (ps_n)^{1-\alpha''_+}$. If $\alpha_0 \geq \sqrt{12}$, then $\alpha''_+ \geq 3$ for suitable $a_+ > 2$. Similarly, we have

$$\begin{aligned}
P_n^+ &= \text{pr}(\hat{I} \notin I_n^+) \\
&\leq \sum_{(j,l) \notin I_n^+} \text{pr}\{\hat{\sigma}_{jl}^2 \geq m^{-1}\sigma^2(1 + \alpha_n)\} \\
&\leq \sum_{(j,l) \notin I_n^+} \text{pr}\{\bar{M}_n \geq m^{-1}\sigma^2(1 + \alpha_n)/(m^{-1}\sigma^2 + \tilde{\sigma}_{jl}^2)\}, \quad \hat{\sigma}_{jl}^2 \sim (m^{-1}\sigma^2 + \tilde{\sigma}_{jl}^2)\chi_n^2/n \\
&\leq ps_n \text{pr}\{\bar{M}_n \geq (1 + \alpha_n)/(1 + (a_- + o(1))\alpha_n)\} \\
&\leq ps_n \text{pr}(\bar{M}_n \geq 1 + \epsilon'_n), \\
&\leq ps_n \exp(-3n\epsilon_n'^2/16),
\end{aligned}$$

where $\epsilon'_n = \{1 - o(1) - a_-\}\alpha_n/\{1 + (o(1) + a_-)\alpha_n\}$ and the third inequality holds because $m(\tilde{\sigma}_{jl}^2 - \sigma_{jl}^2) = o(\alpha_n)$ for all $(j,l) \notin I_n^+$ under Condition 3. We have $n\epsilon_n'^2 \approx \{(1 - a_-)^2\alpha_0^2 \log(ps_n)\}/(1 + a_-\alpha_n)^2 \geq (1 - a_-)^2\alpha' \log(ps_n)$ where α' is slightly smaller than α_0^2 . Let $\alpha''_- = 3(1 - a_-)^2\alpha'/16$, then $P_n^+ \leq (ps_n)^{1-\alpha''_-}$. If $\alpha_0 \geq \sqrt{12}$, then $\alpha''_- > 2$ for suitable $0 < a_- < 1 - \sqrt{8/9}$. By a Borel-Cantelli argument, the result follows from the bounds on P_n^- and P_n^+ . \square

Proof of Lemma 1 and Lemma S1. It is straightforward to obtain the bounds on cardinality of I_n^- and I_n^+ based on sparsity assumptions. Combing Lemma S2 yields the final results. \square

Proof of Theorem S1. On the event A_n , based on the l_0 sparsity, we have

$$E\|\tilde{\mathbf{X}} - \mathbf{X}\|^2 = \sum_{(j,l) \notin \hat{I}} \sigma_{jl}^2 \leq \sum_{(j,l) \notin I_n^-} \sigma_{jl}^2 = O\left\{g\left(\frac{1}{m}\sqrt{\frac{\log p}{n}}\right)^{\frac{2\alpha}{2\alpha+1}}\right\}.$$

According to the result of Theorem 1 in Hall and Hosseini-Nasab (2006),

$$\|\tilde{\boldsymbol{\psi}}_k - \boldsymbol{\psi}_k\| \leq 8^{1/2}k^{a+1} \left[\int \int \sum_{j=1}^p \sum_{j'=1}^p \{\tilde{G}_{jj'}(s,t) - G_{jj'}(s,t)\}^2 ds dt \right]^{1/2}.$$

So, with (S3), we have

$$\|\tilde{\boldsymbol{\psi}}_k - \boldsymbol{\psi}_k\| = O\left\{k^{a+1}g\left(m^{-1}\sqrt{\log p/n}\right)^{\frac{\alpha}{2\alpha+1}}\right\}, \quad a.s..$$

\square

Proof of Theorem S2. Recall that g_n denotes the number of retained processes. Under the weak l_q sparsity, we consider to bound the terms in (S4) replacing g by g_n . Combining (S5) and (S7), using Cauchy-Schwarz inequality and Chebyshev's inequality, we may prove that

$$\begin{aligned} I &= \sum_{j=1}^g \sum_{j'=1}^g \int \int \left[n^{-1} \sum_{i=1}^n \{ \tilde{x}_{ij}(s) - \tilde{x}_{ij}(s) \} \tilde{x}_{ij'}(t) \right]^2 ds dt \\ &= O_p(g^2 m^{-2}). \end{aligned}$$

With (S6) and (S7), we have $II = O_p(g^2 m^{-2})$. Using Cauchy-Schwarz inequality, we deduce that $III = O_p(g^2 n^{-1})$. Thus, we obtain $\|\hat{G} - \tilde{G}\| = O_p(g n^{-1/2} + g m^{-1})$.

Case 1. If $\gamma > 1/2$, the parametric rate dominates while discretization error is negligible, $\|\hat{G} - \tilde{G}\| = O_p(g n^{-1/2})$.

With similar arguments as proof of Theorem 2, we have $\tilde{\lambda}_k - \tilde{\lambda}_{k+1} \geq C k^{-a-1}$, $k = 1, \dots, r_n$ and $\|\hat{\boldsymbol{\psi}}_k - \tilde{\boldsymbol{\psi}}_k\|^2 \leq 8 \sum_{l:l \neq k} (\tilde{\lambda}_k - \tilde{\lambda}_l)^{-2} \left\{ \int \tilde{\boldsymbol{\psi}}_k^\top (\tilde{G} - \hat{G}) \tilde{\boldsymbol{\psi}}_l \right\}^2$, by analogy to (5.22) in Hall and Horowitz (2007), $E \left[\sum_{l:l \neq k} (\tilde{\lambda}_k - \tilde{\lambda}_l)^{-2} \left\{ \int \tilde{\boldsymbol{\psi}}_k^\top (\tilde{G} - \hat{G}) \tilde{\boldsymbol{\psi}}_l \right\}^2 \right] = O(k^2 g^2 n^{-1})$ holds uniformly in $k = 1, \dots, r_n$.

Case 2. If $\gamma \leq 1/2$, the discretization error dominates, $\|\hat{G} - \tilde{G}\| = O_p(g m^{-1})$. With the result of Theorem 1 in Hall and Hosseini-Nasab (2006), the final results are established. \square

Proof of Theorems S3 and S5. . For the approximated scores $\tilde{\eta}_k$,

$$\begin{aligned} |\tilde{\eta}_k - \eta_k| &= | \langle \tilde{\mathbf{X}}, \tilde{\boldsymbol{\psi}}_k \rangle_{\mathbb{H}} - \langle \mathbf{X}, \boldsymbol{\psi}_k \rangle_{\mathbb{H}} | \\ &= | \langle \tilde{\mathbf{X}}, \tilde{\boldsymbol{\psi}}_k - \boldsymbol{\psi}_k \rangle_{\mathbb{H}} + \langle \tilde{\mathbf{X}} - \mathbf{X}, \boldsymbol{\psi}_k \rangle_{\mathbb{H}} | \\ &\leq \|\tilde{\mathbf{X}}\| \|\tilde{\boldsymbol{\psi}}_k - \boldsymbol{\psi}_k\| + \|\tilde{\mathbf{X}} - \mathbf{X}\|. \end{aligned}$$

For the approximated curves $\tilde{\mathbf{X}}^{r_n}$,

$$\begin{aligned} \|\tilde{\mathbf{X}}^{r_n} - \mathbf{X}^{r_n}\| &= \left\| \sum_{k=1}^{r_n} (\tilde{\eta}_k \tilde{\boldsymbol{\psi}}_k - \eta_k \boldsymbol{\psi}_k) \right\| \\ &\leq \left\| \sum_{k=1}^{r_n} \eta_k (\tilde{\boldsymbol{\psi}}_k - \boldsymbol{\psi}_k) \right\| + \left\| \sum_{k=1}^{r_n} \tilde{\boldsymbol{\psi}}_k (\tilde{\eta}_k - \eta_k) \right\| \\ &\leq \sum_{k=1}^{r_n} |\eta_k| \|\tilde{\boldsymbol{\psi}}_k - \boldsymbol{\psi}_k\| + \left\{ \sum_{k=1}^{r_n} (\tilde{\eta}_k - \eta_k)^2 \right\}^{1/2}. \end{aligned}$$

Under the l_0 sparsity, $\|\tilde{\mathbf{X}}\| = O_p(g)$ and under the weak l_q sparsity $\|\tilde{\mathbf{X}}\| = O_p(1)$. According to Theorems 1 and Theorem S1, we establish the results in Theorems S3 and S5.

□

Proof of Theorems S4 and S6. For the estimated scores, we have

$$|\tilde{\eta}_k - \hat{\eta}_k| \leq \|\tilde{\mathbf{X}}\| \|\tilde{\boldsymbol{\psi}}_k - \hat{\boldsymbol{\psi}}_k\| + |\mathbf{u}_k^T(\boldsymbol{\theta}_{\hat{I}} - \hat{\boldsymbol{\theta}}_{\hat{I}})|.$$

where \mathbf{u}_k is the k th eigenvector of $\Sigma = E(\boldsymbol{\theta}_{\hat{I}}\boldsymbol{\theta}_{\hat{I}}^T)$ and the inequality follows from Proposition 1. To quantify the second term in the righthand, we have $|\theta_{jl} - \hat{\theta}_{jl}| = O_p(m^{-1/2})$ for all j, l by simple calculation.

Note that $\tilde{\lambda}_k u_{kjl}^2 \leq \sigma_{jl}^2$. Under l_0 sparsity, we assume $\alpha > 1/2$, then we have $\|\mathbf{u}_k\|_1 = O(k^{\alpha/2}g)$. Thus, $|\mathbf{u}_k^T(\boldsymbol{\theta}_{\hat{I}} - \hat{\boldsymbol{\theta}}_{\hat{I}})| = O_p(k^{\alpha/2}gm^{-1/2})$.

Under weak l_q sparsity, we assume $\alpha > 1/2$ and we consider the most interesting case where $0 < q < 1$. We have $\|\mathbf{u}_k\|_1 = O(k^{\alpha/2})$, then we have $|\mathbf{u}_k^T(\boldsymbol{\theta}_{\hat{I}} - \hat{\boldsymbol{\theta}}_{\hat{I}})| = O_p(k^{\alpha/2}m^{-1/2})$.

We have $\|\tilde{\mathbf{X}}\| = O_p(g)$ under l_0 sparsity and $\|\tilde{\mathbf{X}}\| = O_p(1)$ under weak l_q sparsity. According to the results in Theorems 2 and Theorem S2, we establish results in Theorems S4 and S6.

□